https://dx.doi.org/10.1016/j.yexcr.2022.113042

Preclinical mouse models of hepatocellular carcinoma: An overview and update

Catherine Yujia GU[1], Terence Kin Wah LEE[1,2#]

[1] Department of Applied Biology and Chemical Technology, The Hong Kong Polytechnic University; [2] State Key Laboratory of Chemical Biology and Drug Discovery, The Hong Kong Polytechnic University

[#]Corresponding author:
Dr. Terence K.W. Lee, Room 805, Block Y, Department of Applied Biology and Chemical Technology, Lee Shau Kee Building, The Hong Kong Polytechnic University, Hong Kong.
Tel: (852) 3400-8799; Fax: (852) 2364-9932; Email: terence.kw.lee@polyu.edu.hk

Declaration of competing interests

The authors who have taken part in this study declared that they do not have anything to disclose regarding funding or conflict of interest with respect to this manuscript.

Acknowledgements: This study was supported by RGC General Research Fund (15102020), Collaborative Research Fund (C7026-18G), National Natural Science Foundation of China (82073275) and Research Impact Fund (R5050-18F).

Abstract

Hepatocellular carcinoma (HCC) is by far the most common histological subtype of primary liver cancer. HCC often originates from chronic liver injuries and inflammation, subsequently leading to fibrosis and cirrhosis. Preclinical animal models, especially mice, are viewed as valuable and reliable tools for investigating the molecular processes involved in hepatocarcinogenesis and facilitating the evaluations of the efficacy of novel therapies for HCC. A wide range of mouse models of HCC has been established using various approaches including chemotoxic agents, genetic modifications, special diet administration, and tumor cells transplantation. Choosing a suitable model to represent certain genetic and physiological features of human HCC seems to be crucial. Here, we review the current preclinical mouse models that are frequently used to study HCC.

Keywords: hepatocellular carcinoma; liver cancer; mouse models; preclinical models

1. Introduction

Hepatocellular carcinoma (HCC) is the most common type of primary liver cancer and the third leading cause of cancer-related mortality worldwide [1-3]. The major risk factors for HCC include (1) liver cirrhosis; (2) chronic hepatitis B virus (HBV) or hepatitis C virus (HCV) infections; (3) alcoholic liver disease (ALD); (4) nonalcoholic fatty liver disease (NAFLD); and (5) carcinogen exposure such as aflatoxin-contaminated food [4, 5]. Despite the significant progress in HCC prevention and screening, over 50% of patients are diagnosed with HCC at the advanced or terminal stage, making surgical resection or liver transplantation unavailable as a therapeutic option [6, 7]. In recent years, molecular targeted therapies have been developed for patients with advanced and unresectable HCC [8]. Among them, sorafenib, a multiple-target tyrosine kinase inhibitor, is the current FDA-approved front-line therapeutic intervention, but it can only prolong survival by approximately 3 months [9-11]. More recently, immune checkpoint inhibitors, which mainly block the activity of immune checkpoint proteins

such as programmed cell death protein 1 (PD-1) and programmed death-ligand 1 (PD-L1), have been approved by the FDA as treatments for advanced HCC, but only a small proportion of patients (20%) respond well to the immunotherapies [12-14]. Thus, novel therapies for HCC with better efficacy are urgently needed.

Preclinical animal models are well-established tools used to investigate disease pathogenesis, identify therapeutic targets and screen for effective drugs, thus playing a key role in cancer research. Despite the existence of many animal models of HCC, laboratory mice (*Mus musculus*) are considered the best due to their short lifespan, small body size, high breeding capacity, and physiological, genetic and molecular similarities to humans [15, 16]. Over the last few decades, substantial progress has been achieved in developing a variety of mouse models that target HCC pathogenesis from different angles. Currently, the available mouse models can be categorized into the following three main groups: genetically modified models, induced models and transplantation models [17, 18]. The induced models can be further categorized into chemically induced models, diet-induced models, and virus-induced models [17]. In this review, we will provide an overview of these commonly used HCC mouse models, describe their methodological basis, summarize their advantages and limitations, and highlight their usage in the most recent findings.

2. Genetically modified mouse models

Genetically engineered mouse (GEM) models enable the activation of oncogenes or inactivation of tumor suppressor genes to promote HCC tumor growth. Hydrodynamic tail vein injection (HTVI), a technique that allows for direct gene delivery into the mouse liver, has been widely utilized for creating liver-specific GEM models [19, 20]. This technique involves a rapid injection of a large volume of the solution (10% of the body weight of the injected mouse) containing DNA plasmids encoding the gene of interest into the mouse lateral tail vein within 5-7 seconds [19, 21-24] (Fig. 1). The injected solution directly enters the inferior vena cava and induces transient heart dysfunction and cardiac congestion, which forces the solution out of the endothelium

and into the large hepatic vein in a retrograde movement [20, 25]. The enormous hydrodynamic pressure generated by the rapid injection enlarges the fenestrae of liver sinusoids, increases the permeability of the capillary endothelium and creates transient membrane pores, which allow the DNA plasmids to pass through these pores and reach the intracellular compartment of hepatocytes [17, 25]. Although HTVI does cause transient dysfunction of the cardiac system and structural deformation of the liver, the restoration of normal cardiac and liver functions occurs approximately one week after the injection, and the long-term health conditions of the mice are not affected [20, 26, 27]. Table 1 lists some examples of liver-specific GEM models by using HTVI delivery method based on the most recent findings in the HCC field.

2.1 *Sleeping beauty* transposon system

One main problem of HTVI is that the long-term gene expression in hepatocytes is difficult to maintain because the plasmids delivered to hepatocytes will be gradually degraded and the gene expression will eventually turn off [25, 28, 29]. The *sleeping beauty* (SB) transposon system, one of the DNA recombination technologies, is often used together with HTVI to overcome this problem because it enables the chromosomal integration of the gene of interest and their stable expression in hepatocytes [30, 31]. The SB transposon system requires two plasmids: one plasmid encodes the SB transposase, and the other plasmid functions as a transposon, encoding the gene of interest flanked by two inverted/direct repeat sequences (IR/DRs) [21, 32]. These two plasmids need to be co-injected and hydrodynamically delivered to the liver. During SB-mediated transposition, the SB transposase binds to the IR/DRs of the transposons, excises the transposons containing the gene of interest at the sites of IR/DRs and randomly integrates them into the host genome [23, 32]. The SB transposon system together with HTVI is commonly used to integrate oncogenes into the mouse genome for their constitutive overexpression and subsequent induction of HCC development.

2.2 CRISPR-Cas9 system

As the SB transposon system is often employed to perform gene knock-in, a recent breakthrough in the gene-editing technique known as the CRISPR-Cas9 system can offer sequence-specific gene knockout [33]. The CRISPR-Cas9 system possesses two components: a guide RNA (gRNA) and a Cas9 endonuclease [34, 35]. gRNA guides Cas9 to create double-strand breaks (DSBs) in the target DNA [35]. The error-prone non-homologous end joining (NHEJ) DNA repair mechanism is usually utilized by cells to repair DSBs [36]. Therefore, many mutations are introduced during NHEJ in the form of small deletions or insertions, which results in the loss of gene function and gene knockout. Importantly, HTVI enables the delivery of CRISPR-Cas9 to mouse liver to precisely knock out tumor suppressor genes and induce HCC tumor formation.

2.3 Cre-loxP recombination system

The Cre-loxP recombination system is a powerful site-specific genetic manipulation tool because it allows DNA modification in a specific organ or tissue [16, 31]. The delivery of Cre recombinase by using HTVI allows Cre-loxP-mediated conditional knockout in the mouse liver [37]. In a newly published paper, Liang et al. utilized the Cre-loxP technique to determine the functional role of T-box protein 3 (TBX3) in liver tumorigenesis [38]. They examined the effect of TBX3 ablation on c-Met/ΔN90-β-catenin-mediated hepatocarcinogenesis *in vivo* [38].

2.4 Strengths and limitations of HTVI

HTVI is a simple, elegant and inexpensive approach for liver transgenesis [21-23, 26]. This method is highly specific for hepatocytes, and thus it is useful for liver-specific genetic alterations [22, 26]. In addition, HTVI allows the generation of various HCC models expressing several different oncogenes in a time- and cost-effective manner [22, 25]. Furthermore, HTVI is performed in 6- to 8-week-old adult mice so that mouse embryonic development is not affected, which avoids the troubles that often occur when developing traditional transgenic mouse models [17]. Lastly, the transfection

efficiency of HTVI is approximately 10-40% of hepatocytes [21], so genes in a small proportion of hepatocytes are targeted and altered, which well resembles the initiation of human HCC [25]. Nevertheless, the evidence from microscopic studies shows that the peri-central region of the liver is primarily targeted by HTVI [28]; therefore, studies of tumors originating from other parts of the liver are not feasible. Another limitation of HTVI is that the study results might be affected by the stress and pain caused by the restraint of the mice during HTVI [39]. Therefore, the duration of HTVI should be limited to minimize the suffering of mice.

3. Induced mouse models

3.1 Chemically induced models

Due to inevitable exposure to chemicals exerting toxicity and carcinogenicity in daily life and the essential function of the liver in xenobiotic detoxification, the liver is predisposed to severe damage [17, 57, 58]. Several mouse models have been well established to induce HCC tumorigenesis using chemotoxic agents. These agents can be classified into two main groups: genotoxic and non-genotoxic carcinogens [16, 59]. Genotoxic carcinogens act as tumor initiators to induce hepatocarcinogenesis through direct DNA damage [21, 31, 60]. More specifically, they can directly interact with DNA and form DNA-carcinogen complexes (DNA adducts), which disrupt the DNA structure and produce cancer-promoting mutations [18]. Unlike genotoxic carcinogens, non-genotoxic carcinogens do not interact with DNA. Instead, they function as tumor promoters to enhance tumor formation by disrupting the cellular structure, stimulating malignant cell transformation, and promoting the clonal expansion of preneoplastic cells [31, 59-61]. Chemically induced HCC models often involve a genotoxic carcinogen as an initiator and a non-genotoxic carcinogen as a tumor promoter [15]. The most frequently used genotoxic carcinogen is diethylnitrosamine (DEN), followed by 2-acetylaminofluorene (2-AAF) and aflatoxin [57, 62]. Commonly used non-genotoxic carcinogens include carbon tetrachloride (CCl_4), thioacetamide (TAA) and phenobarbital (PB) [16, 59]. Table 2 lists some examples of chemically

induced mouse models used in recent HCC research.

3.1.1 Genotoxic carcinogens

DEN is the most widely used genotoxic agent for inducing HCC in preclinical research due to its high success rate [63]. The carcinogenesis of DEN involves two stages. Firstly, after the administration of DEN to mice, DEN primarily targets the liver, where it is bioactivated by cytochrome P450 enzymes in centrilobular hepatocytes [64]. Activated DEN acts as an alkylating agent to link two guanine bases of DNA molecules by adding an alkyl group between them, leading to DNA strand breakage and mutagenic DNA adduct formation [16, 63]. Secondly, the activated DEN induces the generation of reactive oxygen species (ROS), which is a threat to DNA stability [17, 65]. The subsequent necrosis and regeneration of hepatocytes promote mutations, neoplastic transformation and ultimately hepatocarcinogenesis [16, 66]. An effective protocol for establishing DEN-induced HCC models involves the administration of a single intraperitoneal injection of DEN (~25 mg/kg body weight) to the mice (less than two weeks old), leading to the occurrence of liver tumor formation at approximately 7-11 months [57]. However, the carcinogenic effects of DEN-induced HCC models vary with age, gender, strain, and administration dosage [18, 59].

3.1.2 Non-genotoxic carcinogens

CCl_4

CCl_4 is a potent hepatotoxin that has been extensively used to induce liver fibrosis in mice [17, 67]. CCl_4-induced hepatotoxicity involves two phases. Firstly, trichloromethyl free radicals are generated when CCl_4 is metabolized by cytochrome P450 [15, 59]. These radicals increase ROS level, which causes peroxidative degradation of membrane phospholipids in hepatocytes and leads to impaired cell membrane integrity [16, 65, 68]. ROS also cause the necrosis and apoptosis of hepatocytes [69, 70]. Secondly, CCl_4 promotes the activation of Kupffer cells that subsequently secrete various cytokines, chemokines and other pro-inflammatory factors in the liver [71]. These pro-inflammatory molecules attract neutrophils, lymphocytes and monocytes

to infiltrate into the inflammation site, which exacerbates liver inflammation and results in liver tissue damage [59]. In contrast to DEN that only requires a single administration, prolonged administration of CCl_4 is necessary because only repeated cycles of injury, inflammation and repair can develop fibrosis and cirrhosis [60]. CCl_4 is commonly administered at a dose of 0.5-2 ml/kg body weight via weekly or biweekly intraperitoneal injections to generate fibrosis in 4-6 weeks [17].

TAA

TAA, another potent centrilobular hepatotoxin, generates sulfine and sulfene metabolites during its bioactivation by a mixed-function oxidase system [72, 73]. These metabolites can modify proteins and amine lipids to initiate hepatic centrilobular necrosis [74, 75]. Repeated administration of TAA either by intraperitoneal injection (100-200 mg/kg body weight) three times a week for 4-8 weeks or in the drinking water (200-500 mg/L) for 6-18 weeks can induce robust fibrosis in mice within 10-15 weeks [76, 77].

PB

Similar to other non-genotoxic carcinogens, PB can induce oxidative stress by increasing cytochrome P450 activity [60, 78]. The unique property of PB-mediated carcinogenesis is that it can induce hypermethylation in the promoter region of tumor suppressor genes, thus inhibiting the expression of tumor suppressor genes and in turn promoting liver tumor development [79, 80]. Therefore, a differential methylation level between mouse strains might be responsible for the different responses to PB. In addition, PB might influence cell proliferation and intracellular signaling [60]. PB is usually administered orally in drinking water or diet to mice over a prolonged period [81, 82]. However, the effect of chronic PB treatment on liver tumor development seems controversial. Braeuning et al. documents that PB exerts tumor-promoting and tumor-inhibitory effects on the growth of hepatocellular adenoma (HCA) and HCC, respectively [83]. This indicates that a more differentiated view of PB-induced liver

tumor growth is necessary.

3.1.3 Two-stage models

Although a single intraperitoneal injection of DEN can induce HCC, the DEN-induced HCC mouse model does not seem to develop the features of fibrosis and cirrhosis that occur in most patients with HCC [57]. These features can be achieved by establishing a two-stage model initiated with a genotoxic compound such as DEN and promoted with a non-genotoxic compound acting as a pro-fibrogenic agent such as CCl_4, TAA and PB [59, 60]. The involvement of fibrogenesis during HCC development more realistically recapitulates the process of HCC pathogenesis and better mimics the tumor microenvironment of human HCC [57].

Overall, chemically induced models mimic the genetic, immunological and environmental features of human HCC, including DNA damage, inflammatory responses, and fibrotic tumor microenvironment [15, 18]. On the other hand, although various combinations of carcinogens have been employed to shorten the time for tumor induction, hepatocarcinogenesis still takes many months to develop [62]. Another drawback of chemically induced models is that the genetic background of the developed tumor is difficult to identify [15, 18].

3.2 Diet-induced mouse models

3.2.1 NAFLD and NASH

Due to a sedentary lifestyle and overconsumption of processed food and fructose-containing beverages, nonalcoholic fatty liver disease (NAFLD) has become a major cause of chronic liver diseases and HCC worldwide [99, 100]. Studies have shown that obesity, insulin resistance, and metabolic syndrome characterized by hypertension, hypertriglyceridemia and hyperlipidemia are responsible for the development of NAFLD [101-105]. The clinical histological manifestation of NAFLD is steatosis in over 5% of hepatocytes [106-108]. The advanced form of NAFLD, nonalcoholic steatohepatitis (NASH), is often associated with fibrosis that may lead to progression

to cirrhosis and eventually HCC [108, 109]. The mechanisms of NASH to HCC progression have been considered multifactorial, including inflammatory cytokines, lipid accumulation, mitochondrial dysfunction and gut microbiota [110]. The initiation of NASH pathogenesis is adequately explained by the "two-hit" hypothesis: lipid droplet accumulation in the liver (a first hit) needs to be accompanied by oxidative stress, ER stress, or necro-inflammation (a second hit), triggering liver inflammation and damage [110, 111].

Diet-induced mouse models have been developed to represent the pathological and metabolic liver alterations observed in human NASH-driven HCC, thereby facilitating development of novel therapeutic strategies. To induce NAFLD, mice are usually fed one or two of the following diets *ad libitum*: high-fat diet (HFD), high-fat high-cholesterol diet (HFHCD), high-fat high-fructose diet (HFHFD), Western diet (WD), choline-deficient high-fat diet (CDHFD), methionine and choline-deficient diet (MCD) and choline-deficient L-amino acid-defined diet (CDAAD) [16, 111-113].

3.2.2 NASH-associated HCC models

In order to induce HCC tumorigenesis, a hepatotoxin can be added to diet-induced models [16]. Table 3 shows some examples of NASH-associated HCC models generated using a hepatotoxin-diet formula. Commonly, 2-week-old C57BL/6 male mice are intraperitoneally injected with DEN and then fed a HFD, CDAAD, CDHFD or WD for 6-9 months, leading to the formation of HCC tumors [114, 115]. Liang et al. reported that the addition of cholesterol to a HFD (HFHCD) after DEN administration led to an increased HCC incidence (90% in HFD-fed mice vs. 100% in HFHCD-fed mice), mainly through mutations in calcium signaling and dysregulated metabolism [116].

3.2.3 Obesogenic mouse models

ob/ob and db/db mice

Leptin, a peptide hormone secreted primarily by white adipose tissue, plays a crucial

role in regulating food intake and body mass [117]. *ob/ob* mice carry mutations in the gene responsible for leptin production, and thus these mice are deficient in functional leptin [118]. Unlike *ob/ob* mice, *db/db* mice carry a point mutation in the leptin receptor gene, which causes a leptin receptor deficiency and defective leptin signaling [118]. Although *ob/ob* and *db/db* mice have different genetic backgrounds, their phenotypes appear to be similar: they have an abnormally increased appetite for food, and therefore they easily become obese and rapidly develop insulin resistance, fatty liver and NAFLD [112]. Importantly, a second stimulus such as DEN needs be added for *ob/ob* and *db/db* mice to develop HCC [111, 119]. One limitation of using *ob/ob* and *db/db* mice is that gene mutations present in these mice are rare in obese humans [110].

ALIOS mice

The American lifestyle-induced obesity syndrome (ALIOS) model was created by Tetri et al. to closely resemble the living habits of modern people: a sedentary lifestyle concurrent with high consumption of fast food [120]. In the ALIOS model, mice are fed a diet high in trans fats and high fructose corn syrup, and the mouse cage rack is removed to promote sedentary behavior and low energy expenditure [21, 120]. The data from Tetri et al. revealed the development of inflammation, severe hepatic steatosis and necrosis after 16 weeks [120]. Another study performed by Dowman et al. showed that mice fed the ALIOS diet displayed histological features of advanced NASH and hepatocellular neoplasms for an extended period of 12 months [121].

STAM mice

An animal model of NASH-related liver carcinogenesis called the Stelic Animal Model (STAM) was developed by Fujii et al. [122]. Two-day-old neonatal C57BL/6 male mice are subcutaneously injected with low-dose streptozotocin (STZ), followed by HFD starting at 4 weeks old to establish STAM [122, 123]. STZ is commonly used to induce type 1 diabetes in preclinical settings because STZ can trigger pancreatic insulin-

producing β cell death, resulting in hyperglycemia and hypoinsulinemia [110]. Notably, when STZ is administered alone, no HCC tumors form, highlighting the necessity of an additional stimulus such as a HFD [124]. The data from the study by Fujii et al. showed that hepatic steatosis, a hallmark of NAFLD, appeared at 6 weeks, followed by NASH at 8 weeks, fibrosis at 12 weeks and HCC at 20 weeks [122]. STAM mice have been widely adopted due to the rapid development of HCC and the resemblance of disease development in humans, but STAM mice that exhibit type 1 diabetes fail to mimic the metabolic syndrome, such as type 2 diabetes and insulin resistance, involved in NASH-driven human HCC [16, 111, 125].

DIAMOND mice

Asgharpour et al. recently developed a stable isogenic B6/129 hybrid strain derived from a cross between C57BL/6J and 129S1/SvImJ mice fed a WD (high fat, high carbohydrate and high cholesterol) together with SW (high fructose-glucose drink), which was named the diet-induced animal model of nonalcoholic fatty liver disease (DIAMOND) mice [126]. DIAMOND mice faithfully recapitulate human NAFLD by developing obesity, insulin resistance and dyslipidemia [112]. They also closely resemble the metabolic, histological, transcriptomic and clinical conditions of humans with NASH and HCC [31, 110]. Hepatic steatosis developed 4-8 weeks after starting the WD-SW diet, followed by fibrosis at 16 weeks, steatohepatitis at 16-24 weeks, and hepatocarcinogenesis in 89% of the mice at 32-52 weeks [126].

MUP-uPA mice

Nakagawa et al. established a diet-induced model of NASH-driven HCC by feeding a HFD to major urinary protein-urokinase plasminogen activator (MUP-uPA) transgenic mice that specifically express an excessive amount of uPA in hepatocytes [127]. The overexpression of uPA induces hepatocyte-specific ER stress and transient liver damage, both of which have been strongly implicated in the pathological features of human NASH [128]. At 24 weeks, HFD-fed MUP-uPA mice exhibited classic hallmarks

of NASH, including steatosis, hepatocyte ballooning and inflammatory infiltrates, all of which displayed similar patterns observed in humans with NASH [127]. At 32-40 weeks, NASH-like disease in HFD-fed MUP-uPA mice spontaneously progressed to HCC [127]. Overall, the HFD-fed MUP-uPA model sufficiently recapitulates several hallmarks of human NASH/HCC disease progression, facilitating studies designed to identify molecular drivers of HCC progression.

3.2.4 Alcoholic liver disease-associated HCC models

Alcoholic liver disease (ALD) is one of the most prevalent liver diseases in many developed countries due to chronic alcohol overconsumption [129]. The spectrum of ALD starts with alcoholic fatty liver (AFL) characterized by hepatic steatosis, which may further progress to alcoholic steatohepatitis (ASH). Similar to the histological features of NASH, ASH is presented as hepatic inflammation, hepatocyte ballooning and liver damage [130]. With continuous liver inflammation and injury, ASH can slowly progress to fibrosis and cirrhosis, which ultimately drives HCC development in some cases [130]. The metabolic pathway of alcohol in hepatocytes involves the generation of acetaldehyde and ROS [31, 129]. Acetaldehyde-mediated carcinogenicity and ROS-mediated DNA damage and lipid peroxidation drive the development of ALD [31, 131]. ALD-associated HCC models commonly include a diet containing alcohol in the form of ethanol combined with a chemical carcinogen (Table 3).

3.3 Virus-induced mouse models

The host tropism of HBV and HCV is highly restricted [7]. Productive infection is limited to humans and chimpanzees [145]. The use of chimpanzees as an animal model faces several limitations, such as a high cost, long lifespan and ethical issues, which impedes their utility in research [7]. Although mice cannot be naturally infected by HBV or HCV, the development of transgenic mouse models carrying certain viral genes makes them more feasible for *in vivo* studies of virus-associated hepatocarcinogenesis [59, 146].

3.3.1 HBV-associated HCC models

HBV is an enveloped DNA virus that exclusively infects hepatocytes [147]. HBV comprises a partially double-stranded circular DNA genome encoding four HB viral proteins: preS/S, preC/C, P and X [148]. HBV X (HBx) protein is commonly used to induce HCC in transgenic mice [146, 149]. Koike et al. generated the first transgenic mice expressing a high level of HBx, and successful HCC tumor formation was observed in 84% of male transgenic mice aged 13-24 months [150]. An analysis of the DNA content in these mice suggested that persistent HBx expression promoted DNA synthesis, which provided a window of genetic mutations in a large number of hepatocytes for malignant transformation. In addition to HBx, Chisari et al. established a transgenic mouse model overexpressing the large envelope polypeptide of hepatitis B surface antigen (HBsAg) [151]. Overexpression of the large envelope polypeptide resulted in the accumulation of long filamentous HBsAg within the endoplasmic reticulum of hepatocytes, leading to hepatotoxicity and carcinogenesis. This early and important study indicates that the expression of a single structural viral component is sufficient to induce malignant transformation [151].

3.3.2 HCV-associated HCC models

HCV is a small enveloped RNA virus consisting of a positive-sense single-stranded RNA genome, capsid protein (core) and envelope glycoproteins 1 & 2 (E1 & E2) [152]. HCV is unlikely to integrate its genetic material into the host genome, and thus researchers postulate that HCV contributes to HCC development through the cumulative effects of chronic infection, inflammation, injury and repair over several decades [153]. Evidence from published studies shows that HCV structural proteins have the potential to trigger hepatic carcinogenesis [15, 62]. For instance, Kamegaya et al. developed two transgenic mice: one expressing only the core protein and the other expressing both the core protein and E1/E2 proteins [154]. Both models developed HCC tumors, but a higher tumor burden was observed in core-E1/E2 transgenic mice [154].

4. Transplantation mouse models

4.1 Xenograft models

The classical xenograft models are established by implanting cultured human HCC cell lines or a fragment of human solid tumor into immunodeficient mice, either under the skin (ectopic) or into the liver (orthotopic) [16, 17, 31, 57]. As xenograft models utilize human cells or tumor tissue carrying human genetic materials, the mutations and properties of human cancer are well preserved [17]. Importantly, xenograft models require the usage of immunodeficient mice to avoid the rejection of transplanted human cells or tumors by the murine immune system [15, 16, 31]. Two frequently used types of immunodeficient mice are athymic nude mice lacking T cells and non-obese diabetic/severe combined immunodeficiency (NOD/SCID) mice harboring very limited innate and adaptive immunity [62, 155, 156]. As immunodeficient mice do not possess a fully functional immune system, the involvement of immune cells in mounting anti-tumor immune responses is limited [18]. Moreover, cytokines and chemokines produced by immune cells within the tumor microenvironment to regulate tumorigenesis are missing [157]. Therefore, these limitations of xenograft models make them unsuitable for the investigation of oncologic immunotherapy.

4.1.1 Cell line ectopic xenograft model

The cell line ectopic xenograft model has been well established in the HCC field for decades [18, 62]. The subcutaneous injection of human HCC cell lines is simple to perform and highly reproducible [62, 158, 159]. In addition, visible tumors can rapidly develop within a few weeks [15]. The subcutaneous implantation enables accurate measurements of tumor size, direct monitoring of tumor progression and easy detection of responses to various treatments [160]. In addition, this model also provides an opportunity to study *in vitro* pre-treated cells [161]. Therefore, the advantages of this model mentioned above make it a compelling preclinical model for anti-cancer drug screening. Nevertheless, the results obtained with this model may not be adequate for predicting human clinical outcomes [57]. One of the major

reasons is that this model lacks hepatic tumor microenvironment, as the liver fibrotic tissue, vascular tissue and stromal tissue are completely absent [162]. Secondly, the *in vitro* culture environment of human HCC cell lines is very different from the *in vivo* living environment of human HCC [158]. Therefore, the phenotypic and genotypic characteristics of HCC cell lines tend not to be representative of tumor cells derived from patients with HCC [158]. Thirdly, the inoculation of one single cell line into immunodeficient mice cannot faithfully recapitulate tumor cell heterogeneity in the bulk of tumors, indicating the necessity of testing multiple cell lines when screening new anticancer drugs to avoid misleading results [17, 59].

4.1.2 Cell line orthotopic xenograft model

In the cell line orthotopic xenograft model, intrahepatic, intrasplenic or intraportal injection is used to establish hepatic tumors (Fig. 2A) [16, 31, 158]. Compared with the ectopic model, this orthotopic model seems to be superior, as it more accurately reflects the native tumor microenvironment, particularly the effects of liver vascularization and dynamic interactions with immune cells and stromal tissue [157, 160]. In addition, this model is able to develop tumor metastasis, thus providing a platform for studies of late stages of liver metastasis [162]. Regarding the disadvantages of this model, tumor growth and progression tend to be more difficult to monitor [57]. With the advances in imaging techniques, the established luciferase-expressing human HCC cell lines enable the tracking of tumor growth in the orthotopic model using *in vivo* bioluminescence imaging [62, 163]. Another drawback is that the orthotopic model is more technically cumbersome due to the requirement for surgical expertise [16, 31].

4.1.3 Patient-derived xenograft model

In addition to transplanting cultured human cell lines, surgically resected tumor specimens obtained from a patient can also be ectopically or orthotopically transplanted into immunodeficient mice, which is termed the patient-derived

xenograft (PDX) model (Fig. 2B) [156, 164]. Notably, PDX could also be established by using patient-derived HCC organoids [160, 165]. The PDX model is considered an effective preclinical cancer model because it closely recapitulates the tumor microenvironment of primary HCC in humans [164, 166, 167]. In addition, the histological, molecular and genetic characteristics of the original HCC biopsies are well retained in the PDX model, thus enabling the prediction of clinical responses to treatment in patients with HCC [156, 160, 166]. Nonetheless, a low engraftment efficiency, long tumorigenesis period and high cost largely limit the wide usage of the PDX model and hinder it from becoming a priority for large-scale drug screening [156, 168].

As the possession of a fully active immune system is essential for testing novel immunotherapies, xenograft models established in immunodeficient mice are unable to reflect the immune response in the tumor, which is a common limitation of xenograft models [18]. In order to test the efficacy of oncologic immunotherapies, numerous efforts have been made to create syngeneic models and humanized mouse models.

4.2 Syngeneic mouse model

The syngeneic model involves the engraftment of mouse cell lines or mouse tumor tissue into immunocompetent mice with the same genetic background through ectopic or orthotopic injection (Fig. 2B) [16, 18, 59]. The use of immunocompetent recipients harboring a complete host immune system allows researchers to study the immunomodulatory effects of anti-cancer drugs [169, 170]. One of the major limitations of syngeneic models is the difference between mice and humans in terms of the genome, immune response and tumor microenvironment [17]. For instance, mutations that occur in mouse HCC tumors may not be relevant to those in primary human HCC.

4.3 Humanized mouse models

The generation of humanized mouse models involves introducing human immune cells into immunodeficient mice to promote the development of a functional human immune system [57]. The commonly used procedure is the transfer of human $CD34^+$ hematopoietic stem cells (HSCs) isolated from fetal cord blood and human peripheral blood mononuclear cells (PBMCs) to the marrow of the mice that have been treated with sublethal irritation (Fig. 2B) [155, 160, 171]. The humanized mouse model can reproduce the complex human immune system and mimic a more realistic tumor microenvironment, enabling the investigation of the efficacy of immunotherapeutic interventions [155]. In addition, a PDX humanized model has been established, involving transplanting human liver tumor samples into humanized mice [172]. Recently, a double humanized mouse model with the humanization of both human immune cells and human hepatocytes has also been developed [16, 31, 173]. In this model, mice possess HSCs and human hepatocytes, which better recapitulates the critical features of dynamic interactions between human HCC tumors and human immune system [170]. Table 4 lists the advantages and disadvantages of transplantation models mentioned above.

5. Conclusions

Overall, the availability of various HCC mouse models has provided researchers opportunities to understand the mechanisms underlying hepatocarcinogenesis (Figure 3). These models have their advantages, limitations and various timepoints of HCC development (Table 5). Nevertheless, no single mouse model can accurately replicate all features found in human HCC. The careful application of a combination of insults may better recapitulate the multifactorial development of HCC in humans. Future trends in HCC research may be related to personalized experimental models that bridge the gap between basic research and clinical application.

Figure Legends

Fig. 1. Schematic diagram of the mechanism of hydrodynamic tail vein injection. DNA plasmids encoding *sleeping beauty* (SB) transposon system or CRISPR-Cas9 system are hydrodynamically injected to the mouse liver. The solution containing DNA plasmids is rapidly injected to the mouse tail vein within 5-7 seconds. The solution enters the inferior vena cava and causes transient cardiac congestion, which successively pushes the solution into the liver in a retrograde movement. IR/DRs: Inverted/direct repeat sequences; EF-1α: Eukaryotic translation elongation factor 1 alpha; CMV: Cytomegalovirus.

Fig. 2. Schematic diagrams of the mechanisms of transplantation mouse models. (A) Illustration of ectopic models established via subcutaneous injection and an orthotopic model generated via intrahepatic, intrasplenic or intraportal injection. **(B)** Xenograft models: a human HCC cell line or human tumor sample is transplanted into immunodeficient mice or humanized mice that are established by introducing human hematopoietic stem cells from fetal cord blood and human peripheral blood mononuclear cells. Syngeneic models: a mouse HCC cell line or mouse tumor sample is transplanted into immunocompetent mice. HCC: Hepatocellular carcinoma.

Figure 3. Schematic diagrams of current HCC mouse models.

(A) Genetically modified models: overexpression of oncogenes via knock-in, inactivation of tumor suppressor gene via knockout, or spatial control of gene expression via Cre-loxP recombination system is able to develop HCC. **(B)** Chemically induced models: carcinogens such as DEN combined with CCl_4, TAA or PB can induce hepatocarcinogenesis in the mouse liver. **(C)** Diet-induced models: oral administration of special diet such as high fat diet can promote NAFLD development. Special diet in combination of DEN can induce NASH-associated HCC tumorigenesis. **(D)** Virus-

induced models: transgenic mouse carrying certain HBV or HCV gene can lead to HCC tumor growth. **(E)** Transplantation models: primary or culture tumor cells can be subcutaneously or orthotopically transplanted to mice to induce tumor formation. HCC: Hepatocellular carcinoma; DEN: Diethylnitrosamine; CCl4: Carbon tetrachloride; TAA: Thioacetamide; PB: phenobarbital; NAFLD: nonalcoholic fatty liver disease; NASH: nonalcoholic steatohepatitis; HBV: hepatitis B virus; HCV: hepatitis C virus.

References

[1] P. Rawla, T. Sunkara, P. Muralidharan, J.P. Raj, Update in global trends and aetiology of hepatocellular carcinoma, Contemp Oncol (Pozn) 22 (2018) 141-150.

[2] E. Kim, P. Viatour, Hepatocellular carcinoma: old friends and new tricks, Exp Mol Med 52 (2020) 1898-1907.

[3] H. Sung, J. Ferlay, R.L. Siegel, M. Laversanne, I. Soerjomataram, A. Jemal, F. Bray, Global Cancer Statistics 2020: GLOBOCAN Estimates of Incidence and Mortality Worldwide for 36 Cancers in 185 Countries, CA Cancer J Clin 71 (2021) 209-249.

[4] A.I. Gomaa, S.A. Khan, M.B. Toledano, I. Waked, S.D. Taylor-Robinson, Hepatocellular carcinoma: epidemiology, risk factors and pathogenesis, World J Gastroenterol 14 (2008) 4300-4308.

[5] D. Janevska, V. Chaloska-Ivanova, V. Janevski, Hepatocellular Carcinoma: Risk Factors, Diagnosis and Treatment, Open Access Maced J Med Sci 3 (2015) 732-736.

[6] A. Gomaa, I. Waked, Management of advanced hepatocellular carcinoma: review of current and potential therapies, Hepatoma Research 3 (2017).

585 [7] Y.C. Teng, Z.Q. Shen, C.H. Kao, T.F. Tsai, Hepatocellular carcinoma mouse models:
586 Hepatitis B virus-associated hepatocarcinogenesis and haploinsufficient tumor
587 suppressor genes, World J Gastroenterol 22 (2016) 300-325.
588 [8] K. Choi, I.H. Baik, S. Ye, Y. Lee, Molecular Targeted Therapy for Hepatocellular
589 Carcinoma Present Status and Future Directions, Biol. Pharm. Bull. 38 (2015) 986-991.
590 [9] M. Kudo, R.S. Finn, S. Qin, K.-H. Han, K. Ikeda, F. Piscaglia, A. Baron, J.-W. Park, G.
591 Han, J. Jassem, J.F. Blanc, A. Vogel, D. Komov, T.R.J. Evans, C. Lopez, C. Dutcus,
592 M. Guo, K. Saito, S. Kraljevic, T. Tamai, M. Ren, A.-L. Cheng, Lenvatinib versus
593 sorafenib in first-line treatment of patients with unresectable hepatocellular carcinoma:
594 a randomised phase 3 non-inferiority trial, The Lancet 391 (2018) 1163-1173.
595 [10] L. Rimassa, A. Santoro, Sorafenib therapy in advanced hepatocellular carcinoma: the
596 SHARP trial, Expert Rev Anticancer Ther 9 (2009) 739-745.
597 [11] A.-L. Cheng, Y.-K. Kang, Z. Chen, C.-J. Tsao, S. Qin, J.S. Kim, R. Luo, J. Feng, S. Ye,
598 T.-S. Yang, J. Xu, Y. Sun, H. Liang, J. Liu, J. Wang, W.Y. Tak, H. Pan, K. Burock, J.
599 Zou, D. Voliotis, Z. Guan, Efficacy and safety of sorafenib in patients in the Asia-Pacific
600 region with advanced hepatocellular carcinoma: a phase III randomised, double-blind,
601 placebo-controlled trial, The Lancet Oncology 10 (2009) 25-34.
602 [12] A.B. El-Khoueiry, B. Sangro, T. Yau, T.S. Crocenzi, M. Kudo, C. Hsu, T.-Y. Kim, S.-P.
603 Choo, J. Trojan, T.H. Welling, T. Meyer, Y.-K. Kang, W. Yeo, A. Chopra, J. Anderson,
604 C. dela Cruz, L. Lang, J. Neely, H. Tang, H.B. Dastani, I. Melero, Nivolumab in patients
605 with advanced hepatocellular carcinoma (CheckMate 040): an open-label, non-
606 comparative, phase 1/2 dose escalation and expansion trial, The Lancet 389 (2017)

607 2492-2502.

608 [13] A.X. Zhu, R.S. Finn, J. Edeline, S. Cattan, S. Ogasawara, D. Palmer, C. Verslype, V.
609 Zagonel, L. Fartoux, A. Vogel, D. Sarker, G. Verset, S.L. Chan, J. Knox, B. Daniele,
610 A.L. Webber, S.W. Ebbinghaus, J. Ma, A.B. Siegel, A.-L. Cheng, M. Kudo, A. Alistar,
611 J. Asselah, J.-F. Blanc, I. Borbath, T. Cannon, K. Chung, A. Cohn, D.P. Cosgrove, N.
612 Damjanov, M. Gupta, Y. Karino, M. Karwal, A. Kaubisch, R. Kelley, J.-L. Van Laethem,
613 T. Larson, J. Lee, D. Li, A. Manhas, G.A. Manji, K. Numata, B. Parsons, A.S. Paulson,
614 C. Pinto, R. Ramirez, S. Ratnam, M. Rizell, O. Rosmorduc, Y. Sada, Y. Sasaki, P.I.
615 Stal, S. Strasser, J. Trojan, G. Vaccaro, H. Van Vlierberghe, A. Weiss, K.-H. Weiss, T.
616 Yamashita, Pembrolizumab in patients with advanced hepatocellular carcinoma
617 previously treated with sorafenib (KEYNOTE-224): a non-randomised, open-label
618 phase 2 trial, The Lancet Oncology 19 (2018) 940-952.

619 [14] R.S. Finn, S. Qin, M. Ikeda, P.R. Galle, M. Ducreux, T.Y. Kim, M. Kudo, V. Breder, P.
620 Merle, A.O. Kaseb, D. Li, W. Verret, D.Z. Xu, S. Hernandez, J. Liu, C. Huang, S. Mulla,
621 Y. Wang, H.Y. Lim, A.X. Zhu, A.L. Cheng, I.M. Investigators, Atezolizumab plus
622 Bevacizumab in Unresectable Hepatocellular Carcinoma, N Engl J Med 382 (2020)
623 1894-1905.

624 [15] P. Newell, A. Villanueva, S.L. Friedman, K. Koike, J.M. Llovet, Experimental models of
625 hepatocellular carcinoma, J Hepatol 48 (2008) 858-879.

626 [16] K. Liu, J. Chen, G.W. McCaughan, Animal models for hepatocellular carcinoma arising
627 from alcoholic and metabolic liver diseases, Hepatoma Res 6 (2020) 7.

628 [17] H.E. Zhang, J.M. Henderson, M.D. Gorrell, Animal models for hepatocellular carcinoma,

Biochim Biophys Acta Mol Basis Dis 1865 (2019) 993-1002.

[18] Z. Macek Jilkova, K. Kurma, T. Decaens, Animal Models of Hepatocellular Carcinoma: The Role of Immune System and Tumor Microenvironment, Cancers (Basel) 11 (2019).

[19] B. Bonamassa, L. Hai, D. Liu, Hydrodynamic gene delivery and its applications in pharmaceutical research, Pharm. Res. 28 (2011) 694-701.

[20] T. Suda, D. Liu, Hydrodynamic gene delivery: its principles and applications, Mol Ther 15 (2007) 2063-2069.

[21] R. Carlessi, J. Köhn-Gaone, J.K. Olynyk, J.E.E. Tirnitz-Parker, Mouse Models of Hepatocellular Carcinoma, Hepatocellular Carcinoma, 2019, pp. 69-94.

[22] H.L. Ju, K.H. Han, J.D. Lee, S.W. Ro, Transgenic mouse models generated by hydrodynamic transfection for genetic studies of liver cancer and preclinical testing of anti-cancer therapy, Int J Cancer 138 (2016) 1601-1608.

[23] H.L. Ju, S.H. Ahn, D.Y. Kim, S. Baek, S.I. Chung, J. Seong, K.H. Han, S.W. Ro, Investigation of oncogenic cooperation in simple liver-specific transgenic mouse models using noninvasive in vivo imaging, PLoS One 8 (2013) e59869.

[24] M. Huang, R. Sun, Q. Huang, Z. Tian, Technical Improvement and Application of Hydrodynamic Gene Delivery in Study of Liver Diseases, Front Pharmacol 8 (2017) 591.

[25] X. Chen, D.F. Calvisi, Hydrodynamic transfection for generation of novel mouse models for liver cancer research, Am J Pathol 184 (2014) 912-923.

[26] S.I. Chung, H. Moon, D.Y. Kim, K.J. Cho, H.L. Ju, D.Y. Kim, S.H. Ahn, K.H. Han, S.W. Ro, Development of a transgenic mouse model of hepatocellular carcinoma with a liver

651 fibrosis background, BMC Gastroenterol 16 (2016) 13.

652 [27] G. Zhang, X. Gao, Y.K. Song, R. Vollmer, D.B. Stolz, J.Z. Gasiorowski, D.A. Dean, D.
653 Liu, Hydroporation as the mechanism of hydrodynamic delivery, Gene Ther 11 (2004)
654 675-682.

655 [28] T. Suda, X. Gao, D.B. Stolz, D. Liu, Structural impact of hydrodynamic injection on
656 mouse liver, Gene Ther 14 (2007) 129-137.

657 [29] J.B. Bell, E.L. Aronovich, J.M. Schreifels, T.C. Beadnell, P.B. Hackett, Duration of
658 expression and activity of Sleeping Beauty transposase in mouse liver following
659 hydrodynamic DNA delivery, Mol. Ther. 18 (2010) 1796-1802.

660 [30] J.B. Bell, K.M. Podetz-Pedersen, E.L. Aronovich, L.R. Belur, R.S. McIvor, P.B. Hackett,
661 Preferential delivery of the Sleeping Beauty transposon system to livers of mice by
662 hydrodynamic injection, Nat. Protoc. 2 (2007) 3153-3165.

663 [31] Z.J. Brown, B. Heinrich, T.F. Greten, Mouse models of hepatocellular carcinoma: an
664 overview and highlights for immunotherapy research, Nat. Rev. Gastroenterol. Hepatol.
665 15 (2018) 536-554.

666 [32] P.B. Hackett, S.C. Ekker, D.A. Largaespada, R.S. McIvor, Sleeping Beauty
667 Transposon-Mediated Gene Therapy for Prolonged Expression, Non-Viral Vectors for
668 Gene Therapy, Second Edition: Part 2, 2005, Vol. 54, pp. 189-232.

669 [33] H. Wang, H. Yang, C.S. Shivalila, M.M. Dawlaty, A.W. Cheng, F. Zhang, R. Jaenisch,
670 One-step generation of mice carrying mutations in multiple genes by CRISPR/Cas-
671 mediated genome engineering, Cell 153 (2013) 910-918.

672 [34] L. Sun, B.M. Lutz, Y. Tao, The CRISPR/Cas9 system for gene editing and its potential

673 application in pain research, Transl Perioper Pain Med. 1 (2016) 22–33.
674 [35] F.A. Ran, P.D. Hsu, J. Wright, V. Agarwala, D.A. Scott, F. Zhang, Genome engineering
675 using the CRISPR-Cas9 system, Nat Protoc 8 (2013) 2281-2308.
676 [36] H.H.Y. Chang, N.R. Pannunzio, N. Adachi, M.R. Lieber, Non-homologous DNA end
677 joining and alternative pathways to double-strand break repair, Nat Rev Mol Cell Biol
678 18 (2017) 495-506.
679 [37] H.Z. Zhu, W. Wang, D.M. Feng, Y. Sai, J.L. Xue, Conditional gene modification in
680 mouse liver using hydrodynamic delivery of plasmid DNA encoding Cre recombinase,
681 FEBS Lett 580 (2006) 4346-4352.
682 [38] B. Liang, Y. Zhou, M. Qian, M. Xu, J. Wang, Y. Zhang, X. Song, H. Wang, S. Lin, C.
683 Ren, S.P. Monga, B. Wang, M. Evert, Y. Chen, X. Chen, Z. Huang, D.F. Calvisi, X.
684 Chen, TBX3 functions as a tumor suppressor downstream of activated CTNNB1
685 mutants during hepatocarcinogenesis, J Hepatol 75 (2021) 120-131.
686 [39] S.C. Gad, Rodents model for toxicity testing and biomarkers, Biomarkers in Toxicology,
687 2014, pp. 7-69.
688 [40] K. Kamimura, T. Yokoo, H. Abe, N. Sakai, T. Nagoya, Y. Kobayashi, M. Ohtsuka, H.
689 Miura, A. Sakamaki, H. Kamimura, N. Miyamura, H. Nishina, S. Terai, Effect of
690 Diphtheria Toxin-Based Gene Therapy for Hepatocellular Carcinoma, Cancers (Basel)
691 12 (2020).
692 [41] A. Cigliano, M.G. Pilo, L. Li, G. Latte, M. Szydlowska, M.M. Simile, P. Paliogiannis, L.
693 Che, G.M. Pes, G. Palmieri, M.C. Sini, A. Cossu, A. Porcu, G. Vidili, M.A. Seddaiu,
694 R.M. Pascale, S. Ribback, F. Dombrowski, X. Chen, D.F. Calvisi, Deregulated c-Myc

requires a functional HSF1 for experimental and human hepatocarcinogenesis, Oncotarget 8 (2017) 90638-90650.

[42] J. Hu, L. Che, L. Li, M.G. Pilo, A. Cigliano, S. Ribback, X. Li, G. Latte, M. Mela, M. Evert, F. Dombrowski, G. Zheng, X. Chen, D.F. Calvisi, Co-activation of AKT and c-Met triggers rapid hepatocellular carcinoma development via the mTORC1/FASN pathway in mice, Sci Rep 6 (2016) 20484.

[43] Y. Mo, Y. Wu, X. Li, H. Rao, X. Tian, D. Wu, Z. Qiu, G. Zheng, J. Hu, Osthole delays hepatocarcinogenesis in mice by suppressing AKT/FASN axis and ERK phosphorylation, Eur J Pharmacol 867 (2020) 172788.

[44] Y. Qiao, M. Xu, J. Tao, L. Che, A. Cigliano, S.P. Monga, D.F. Calvisi, X. Chen, Oncogenic potential of N-terminal deletion and S45Y mutant beta-catenin in promoting hepatocellular carcinoma development in mice, BMC Cancer 18 (2018) 1093.

[45] N. Zhan, A.A. Michael, K. Wu, G. Zeng, A. Bell, J. Tao, S.P. Monga, The Effect of Selective c-MET Inhibitor on Hepatocellular Carcinoma in the MET-Active, beta-Catenin-Mutated Mouse Model, Gene Expr 18 (2018) 135-147.

[46] Y. Li, N. Lin, J. Xu, Y. Lu, S. Chen, C. Pan, C. Wang, M. Xu, B. Zhou, R. Xu, Y.J. Xu, Measurement of Serum and Hepatic Eicosanoids by Liquid Chromatography Tandem-Mass Spectrometry (LC-MS/MS) in a Mouse Model of Hepatocellular Carcinoma (HCC) with Delivery of c-Met and Activated beta-Catenin by Hepatocyte Hydrodynamic Injection, Med Sci Monit 24 (2018) 1670-1679.

[47] J. Tao, E. Xu, Y. Zhao, S. Singh, X. Li, G. Couchy, X. Chen, J. Zucman-Rossi, M. Chikina, S.P. Monga, Modeling a human hepatocellular carcinoma subset in mice

through coexpression of met and point-mutant beta-catenin, Hepatology 64 (2016) 1587-1605.

[48] Y.T. Liu, T.C. Tseng, R.S. Soong, C.Y. Peng, Y.H. Cheng, S.F. Huang, T.H. Chuang, J.H. Kao, L.R. Huang, A novel spontaneous hepatocellular carcinoma mouse model for studying T-cell exhaustion in the tumor microenvironment, J Immunother Cancer 6 (2018) 144.

[49] T. Kido, Z.L. Tabatabai, X. Chen, Y.C. Lau, Potential dual functional roles of the Y-linked RBMY in hepatocarcinogenesis, Cancer Sci 111 (2020) 2987-2999.

[50] K. Cho, S.W. Ro, H.W. Lee, H. Moon, S. Han, H.R. Kim, S.H. Ahn, J.Y. Park, D.Y. Kim, YAP/TAZ Suppress Drug Penetration Into Hepatocellular Carcinoma Through Stromal Activation, Hepatology (2021).

[51] M. Gao, D. Liu, CRISPR/Cas9-based Pten knock-out and Sleeping Beauty Transposon-mediated Nras knock-in induces hepatocellular carcinoma and hepatic lipid accumulation in mice, Cancer Biol Ther 18 (2017) 505-512.

[52] D.K. Chiu, V.W. Yuen, J.W. Cheu, L.L. Wei, V. Ting, M. Fehlings, H. Sumatoh, A. Nardin, E.W. Newell, I.O. Ng, T.C. Yau, C.M. Wong, C.C. Wong, Hepatocellular Carcinoma Cells Up-regulate PVRL1, Stabilizing PVR and Inhibiting the Cytotoxic T-Cell Response via TIGIT to Mediate Tumor Resistance to PD1 Inhibitors in Mice, Gastroenterology 159 (2020) 609-623.

[53] D. Lee, I.M. Xu, D.K. Chiu, J. Leibold, A.P. Tse, M.H. Bao, V.W. Yuen, C.Y. Chan, R.K. Lai, D.W. Chin, D.F. Chan, T.T. Cheung, S.H. Chok, C.M. Wong, S.W. Lowe, I.O. Ng, C.C. Wong, Induction of Oxidative Stress Through Inhibition of Thioredoxin Reductase

1 Is an Effective Therapeutic Approach for Hepatocellular Carcinoma, Hepatology 69 (2019) 1768-1786.

[54] Z. Xu, J. Hu, H. Cao, M.G. Pilo, A. Cigliano, Z. Shao, M. Xu, S. Ribback, F. Dombrowski, D.F. Calvisi, X. Chen, Loss of Pten synergizes with c-Met to promote hepatocellular carcinoma development via mTORC2 pathway, Exp Mol Med 50 (2018) e417.

[55] L. Li, G.M. Pilo, X. Li, A. Cigliano, G. Latte, L. Che, C. Joseph, M. Mela, C. Wang, L. Jiang, S. Ribback, M.M. Simile, R.M. Pascale, F. Dombrowski, M. Evert, C.F. Semenkovich, X. Chen, D.F. Calvisi, Inactivation of fatty acid synthase impairs hepatocarcinogenesis driven by AKT in mice and humans, J Hepatol 64 (2016) 333-341.

[56] L. Che, M.G. Pilo, A. Cigliano, G. Latte, M.M. Simile, S. Ribback, F. Dombrowski, M. Evert, X. Chen, D.F. Calvisi, Oncogene dependent requirement of fatty acid synthase in hepatocellular carcinoma, Cell Cycle 16 (2017) 499-507.

[57] A. Blidisel, I. Marcovici, D. Coricovac, F. Hut, C.A. Dehelean, O.M. Cretu, Experimental Models of Hepatocellular Carcinoma-A Preclinical Perspective, Cancers (Basel) 13 (2021).

[58] Y.L. Lin, Y. Li, Study on the hepatocellular carcinoma model with metastasis, Genes Dis 7 (2020) 336-350.

[59] N.P. Santos, A.A. Colaco, P.A. Oliveira, Animal models as a tool in hepatocellular carcinoma research: A Review, Tumour Biol 39 (2017) 1010428317695923.

[60] F. Heindryckx, I. Colle, H. Van Vlierberghe, Experimental mouse models for hepatocellular carcinoma research, Int J Exp Pathol 90 (2009) 367-386.

761 [61] M.W. Leenders, M.W. Nijkamp, I.H. Borel Rinkes, Mouse models in liver cancer
762 research: a review of current literature, World J Gastroenterol 14 (2008) 6915-6923.
763 [62] L. He, D.A. Tian, P.Y. Li, X.X. He, Mouse models of liver cancer Progress and
764 recommendations, Oncotarget 6 (2015) 23306-23322.
765 [63] Q. Tang, Q. Wang, Q. Zhang, S.Y. Lin, Y. Zhu, X. Yang, A.Y. Guo, Gene expression,
766 regulation of DEN and HBx induced HCC mice models and comparisons of tumor,
767 para-tumor and normal tissues, BMC Cancer 17 (2017) 862.
768 [64] F. Connor, T.F. Rayner, S.J. Aitken, C. Feig, M. Lukk, J. Santoyo-Lopez, D.T. Odom,
769 Mutational landscape of a chemically-induced mouse model of liver cancer, J Hepatol
770 69 (2018) 840-850.
771 [65] Y. Sanchez-Perez, C. Carrasco-Legleu, C. Garcia-Cuellar, J. Perez-Carreon, S.
772 Hernandez-Garcia, M. Salcido-Neyoy, L. Aleman-Lazarini, S. Villa-Trevino, Oxidative
773 stress in carcinogenesis. Correlation between lipid peroxidation and induction of
774 preneoplastic lesions in rat hepatocarcinogenesis, Cancer Lett 217 (2005) 25-32.
775 [66] L. Bakiri, E.F. Wagner, Mouse models for liver cancer, Mol Oncol 7 (2013) 206-223.
776 [67] M. Galicia-Moreno, J.A. Silva-Gomez, S. Lucano-Landeros, A. Santos, H.C. Monroy-
777 Ramirez, J. Armendariz-Borunda, Liver Cancer: Therapeutic Challenges and the
778 Importance of Experimental Models, Can J Gastroenterol Hepatol 2021 (2021)
779 8837811.
780 [68] K.W. Chan, W.S. Ho, Anti-oxidative and hepatoprotective effects of lithospermic acid
781 against carbon tetrachloride-induced liver oxidative damage in vitro and in vivo, Oncol
782 Rep 34 (2015) 673-680.

783 [69] S.A. Sheweita, M. Abd El-Gabar, M. Bastawy, Carbon tetrachloride changes the activity
784 of cytochrome P450 system in the liver of male rats: role of antioxidants, Toxicology
785 169 (2001) 83-92.
786 [70] F. Ozturk, M. Gul, B. Ates, I.C. Ozturk, A. Cetin, N. Vardi, A. Otlu, I. Yilmaz, Protective
787 effect of apricot (Prunus armeniaca L.) on hepatic steatosis and damage induced by
788 carbon tetrachloride in Wistar rats, Br J Nutr 102 (2009) 1767-1775.
789 [71] M.K. Manibusan, M. Odin, D.A. Eastmond, Postulated carbon tetrachloride mode of
790 action: a review, J Environ Sci Health C Environ Carcinog Ecotoxicol Rev 25 (2007)
791 185-209.
792 [72] T. Akhtar, N. Sheikh, An overview of thioacetamide-induced hepatotoxicity, Toxin
793 Reviews 32 (2013) 43-46.
794 [73] P. Stankova, O. Kucera, H. Lotkova, T. Rousar, R. Endlicher, Z. Cervinkova, The toxic
795 effect of thioacetamide on rat liver in vitro, Toxicol In Vitro 24 (2010) 2097-2103.
796 [74] H. Hajovsky, G. Hu, Y. Koen, D. Sarma, W. Cui, D.S. Moore, J.L. Staudinger, R.P.
797 Hanzlik, Metabolism and toxicity of thioacetamide and thioacetamide S-oxide in rat
798 hepatocytes, Chem Res Toxicol 25 (2012) 1955-1963.
799 [75] Y.M. Koen, D. Sarma, H. Hajovsky, N.A. Galeva, T.D. Williams, J.L. Staudinger, R.P.
800 Hanzlik, Protein targets of thioacetamide metabolites in rat hepatocytes, Chem Res
801 Toxicol 26 (2013) 564-574.
802 [76] M.C. Wallace, K. Hamesch, M. Lunova, Y. Kim, R. Weiskirchen, P. Strnad, S.L.
803 Friedman, Standard operating procedures in experimental liver research:
804 thioacetamide model in mice and rats, Lab Anim 49 (2015) 21-29.

[77] M.M. Zaldivar, K. Pauels, P. von Hundelshausen, M.L. Berres, P. Schmitz, J. Bornemann, M.A. Kowalska, N. Gassler, K.L. Streetz, R. Weiskirchen, C. Trautwein, C. Weber, H.E. Wasmuth, CXC chemokine ligand 4 (Cxcl4) is a platelet-derived mediator of experimental liver fibrosis, Hepatology 51 (2010) 1345-1353.

[78] A. Kakehashi, N. Ishii, T. Okuno, M. Fujioka, M. Gi, S. Fukushima, H. Wanibuchi, Progression of Hepatic Adenoma to Carcinoma in Ogg1 Mutant Mice Induced by Phenobarbital, Oxidative Medicine and Cellular Longevity 2017 (2017) 1-16.

[79] J.M. Phillips, J.I. Goodman, Identification of genes that may play critical roles in phenobarbital (PB)-induced liver tumorigenesis due to altered DNA methylation, Toxicol Sci 104 (2008) 86-99.

[80] R.E. Watson, J.I. Goodman, Effects of Phenobarbital on DNA Methylation in GC-Rich Regions of Hepatic DNA from Mice That Exhibit Different Levels of Susceptibility to Liver Tumorigenesis, Toxicological Sciences 68 (2002) 51-58.

[81] N.M. Abdel-Hamid, T.K. Mahmoud, S.A. Abass, M.M. El-Shishtawy, Expression of thioredoxin and glutaredoxin in experimental hepatocellular carcinoma-Relevance for prognostic and diagnostic evaluation, Pathophysiology 25 (2018) 433-438.

[82] H.M. El Miniawy, K.A. Ahmed, S.A. Mansour, M.M. Khattab, In vivo antitumour potential of camel's milk against hepatocellular carcinoma in rats and its improvement of cisplatin renal side effects, Pharm Biol 55 (2017) 1513-1520.

[83] A. Braeuning, A. Gavrilov, M. Geissler, C. Wenz, S. Colnot, M.F. Templin, U. Metzger, M. Romer, A. Zell, M. Schwarz, Tumor promotion and inhibition by phenobarbital in livers of conditional Apc-deficient mice, Arch Toxicol 90 (2016) 1481-1494.

827 [84] A. Esparza-Baquer, I. Labiano, O. Sharif, A. Agirre-Lizaso, F. Oakley, P.M. Rodrigues,
828 E. Zhuravleva, C.J. O'Rourke, E. Hijona, R. Jimenez-Aguero, I. Riano, A. Landa, A. La
829 Casta, M.Y.W. Zaki, P. Munoz-Garrido, M. Azkargorta, F. Elortza, A. Vogel, G.
830 Schabbauer, P. Aspichueta, J.B. Andersen, S. Knapp, D.A. Mann, L. Bujanda, J.M.
831 Banales, M.J. Perugorria, TREM-2 defends the liver against hepatocellular carcinoma
832 through multifactorial protective mechanisms, Gut 70 (2021) 1345-1361.
833 [85] S. Liu, Y. Sun, M. Jiang, Y. Li, Y. Tian, W. Xue, N. Ding, Y. Sun, C. Cheng, J. Li, X.
834 Miao, X. Liu, L. Zheng, K. Huang, Glyceraldehyde-3-phosphate dehydrogenase
835 promotes liver tumorigenesis by modulating phosphoglycerate dehydrogenase,
836 Hepatology 66 (2017) 631-645.
837 [86] L. Bakiri, R. Hamacher, O. Grana, A. Guio-Carrion, R. Campos-Olivas, L. Martinez,
838 H.P. Dienes, M.K. Thomsen, S.C. Hasenfuss, E.F. Wagner, Liver carcinogenesis by
839 FOS-dependent inflammation and cholesterol dysregulation, J Exp Med 214 (2017)
840 1387-1409.
841 [87] M.J. Mittenbuhler, K. Saedler, H. Nolte, L. Kern, J. Zhou, S.B. Qian, L. Meder, R.T.
842 Ullrich, J.C. Bruning, F.T. Wunderlich, Hepatic FTO is dispensable for the regulation of
843 metabolism but counteracts HCC development in vivo, Mol Metab 42 (2020) 101085.
844 [88] L.Z. Wen, K. Ding, Z.R. Wang, C.H. Ding, S.J. Lei, J.P. Liu, C. Yin, P.F. Hu, J. Ding,
845 W.S. Chen, X. Zhang, W.F. Xie, SHP-1 Acts as a Tumor Suppressor in
846 Hepatocarcinogenesis and HCC Progression, Cancer Res 78 (2018) 4680-4691.
847 [89] X. Ma, Y. Qiu, Y. Sun, L. Zhu, Y. Zhao, T. Li, Y. Lin, D. Ma, Z. Qin, C. Sun, L. Han,
848 NOD2 inhibits tumorigenesis and increases chemosensitivity of hepatocellular

carcinoma by targeting AMPK pathway, Cell Death Dis 11 (2020) 174.

[90] J. Li, Q. Wang, Y. Yang, C. Lei, F. Yang, L. Liang, C. Chen, J. Xia, K. Wang, N. Tang, GSTZ1 deficiency promotes hepatocellular carcinoma proliferation via activation of the KEAP1/NRF2 pathway, J Exp Clin Cancer Res 38 (2019) 438.

[91] Y. Zhou, L. Hu, W. Tang, D. Li, L. Ma, H. Liu, S. Zhang, X. Zhang, L. Dong, X. Shen, S. Chen, R. Xue, S. Zhang, Hepatic NOD2 promotes hepatocarcinogenesis via a RIP2-mediated proinflammatory response and a novel nuclear autophagy-mediated DNA damage mechanism, J Hematol Oncol 14 (2021) 9.

[92] G.R. Romualdo, G.B. Prata, T.C. da Silva, A.A.H. Fernandes, F.S. Moreno, B. Cogliati, L.F. Barbisan, Fibrosis-associated hepatocarcinogenesis revisited: Establishing standard medium-term chemically-induced male and female models, PLoS One 13 (2018) e0203879.

[93] A. Memon, Y. Pyao, Y. Jung, J.I. Lee, W.K. Lee, A Modified Protocol of Diethylnitrosamine Administration in Mice to Model Hepatocellular Carcinoma, Int J Mol Sci 21 (2020).

[94] F. Wang, Y. Zhang, J. Shen, B. Yang, W. Dai, J. Yan, S. Maimouni, H.Q. Daguplo, S. Coppola, Y. Gao, Y. Wang, Z. Du, K. Peng, H. Liu, Q. Zhang, F. Tang, P. Wang, S. Gao, Y. Wang, W.X. Ding, G. Guo, F. Wang, W.X. Zong, The Ubiquitin E3 Ligase TRIM21 Promotes Hepatocarcinogenesis by Suppressing the p62-Keap1-Nrf2 Antioxidant Pathway, Cell Mol Gastroenterol Hepatol 11 (2021) 1369-1385.

[95] S.A. Gani, S.A. Muhammad, A.U. Kura, F. Barahuie, M.Z. Hussein, S. Fakurazi, Effect of protocatechuic acid-layered double hydroxide nanoparticles on

diethylnitrosamine/phenobarbital-induced hepatocellular carcinoma in mice, PLoS One 14 (2019) e0217009.

[96] L. Zhang, P. Yang, J. Wang, Q. Liu, T. Wang, Y. Wang, F. Lin, MiR-22 regulated T cell differentiation and hepatocellular carcinoma growth by directly targeting Jarid2, Am J Cancer Res. 11 (2021) 2159-2173.

[97] S.M. Aly, H.A. Fetaih, A.A.I. Hassanin, M.M. Abomughaid, A.A. Ismail, Protective Effects of Garlic and Cinnamon Oils on Hepatocellular Carcinoma in Albino Rats, Anal Cell Pathol (Amst) 2019 (2019) 9895485.

[98] J. Shi, X. Han, J. Wang, G. Han, M. Zhao, X. Duan, L. Mi, N. Li, X. Yin, H. Shi, C. Li, J. Gao, J. Xu, F. Yin, Matrine prevents the early development of hepatocellular carcinoma like lesions in rat liver, Exp Ther Med 18 (2019) 2583-2591.

[99] M.B. Vos, J.E. Lavine, Dietary fructose in nonalcoholic fatty liver disease, Hepatology 57 (2013) 2525-2531.

[100] T. Jensen, M.F. Abdelmalek, S. Sullivan, K.J. Nadeau, M. Green, C. Roncal, T. Nakagawa, M. Kuwabara, Y. Sato, D.H. Kang, D.R. Tolan, L.G. Sanchez-Lozada, H.R. Rosen, M.A. Lanaspa, A.M. Diehl, R.J. Johnson, Fructose and sugar: A major mediator of non-alcoholic fatty liver disease, J Hepatol 68 (2018) 1063-1075.

[101] A.F. Godoy-Matos, W.S. Silva Junior, C.M. Valerio, NAFLD as a continuum: from obesity to metabolic syndrome and diabetes, Diabetol Metab Syndr 12 (2020) 60.

[102] N.M. El-Koofy, G.M. Anwar, M.S. El-Raziky, A.M. El-Hennawy, F.M. El-Mougy, H.M. El-Karaksy, F.M. Hassanin, H.M. Helmy, The association of metabolic syndrome, insulin resistance and non-alcoholic fatty liver disease in overweight/obese children,

Saudi J Gastroenterol 18 (2012) 44-49.

[103] B.N. Finck, Targeting Metabolism, Insulin Resistance, and Diabetes to Treat Nonalcoholic Steatohepatitis, Diabetes 67 (2018) 2485-2493.

[104] S. Scapaticci, E. D'Adamo, A. Mohn, F. Chiarelli, C. Giannini, Non-Alcoholic Fatty Liver Disease in Obese Youth With Insulin Resistance and Type 2 Diabetes, Front Endocrinol (Lausanne) 12 (2021) 639548.

[105] K.C. Yang, H.F. Hung, C.W. Lu, H.H. Chang, L.T. Lee, K.C. Huang, Association of Non-alcoholic Fatty Liver Disease with Metabolic Syndrome Independently of Central Obesity and Insulin Resistance, Sci Rep 6 (2016) 27034.

[106] G.T. Brown, D.E. Kleiner, Histopathology of nonalcoholic fatty liver disease and nonalcoholic steatohepatitis, Metabolism 65 (2016) 1080-1086.

[107] P. Bedossa, Pathology of non-alcoholic fatty liver disease, Liver Int 37 Suppl 1 (2017) 85-89.

[108] T. Hardy, F. Oakley, Q.M. Anstee, C.P. Day, Nonalcoholic Fatty Liver Disease: Pathogenesis and Disease Spectrum, Annu Rev Pathol 11 (2016) 451-496.

[109] F. Piscaglia, G. Svegliati-Baroni, A. Barchetti, A. Pecorelli, S. Marinelli, C. Tiribelli, S. Bellentani, H.-N.I.S. Group, Clinical patterns of hepatocellular carcinoma in nonalcoholic fatty liver disease: A multicenter prospective study, Hepatology 63 (2016) 827-838.

[110] K. Chen, J. Ma, X. Jia, W. Ai, Z. Ma, Q. Pan, Advancing the understanding of NAFLD to hepatocellular carcinoma development: From experimental models to humans, Biochim Biophys Acta Rev Cancer 1871 (2019) 117-125.

915 [111] M.A. Febbraio, S. Reibe, S. Shalapour, G.J. Ooi, M.J. Watt, M. Karin, Preclinical
916 Models for Studying NASH-Driven HCC: How Useful Are They?, Cell Metab 29 (2019)
917 18-26.
918 [112] P.K. Santhekadur, D.P. Kumar, A.J. Sanyal, Preclinical models of non-alcoholic fatty
919 liver disease, J Hepatol 68 (2018) 230-237.
920 [113] K.D. Corbin, S.H. Zeisel, Choline metabolism provides novel insights into nonalcoholic
921 fatty liver disease and its progression, Curr Opin Gastroenterol 28 (2012) 159-165.
922 [114] T. Tsuchida, Y.A. Lee, N. Fujiwara, M. Ybanez, B. Allen, S. Martins, M.I. Fiel, N.
923 Goossens, H.I. Chou, Y. Hoshida, S.L. Friedman, A simple diet- and chemical-induced
924 murine NASH model with rapid progression of steatohepatitis, fibrosis and liver cancer,
925 J Hepatol 69 (2018) 385-395.
926 [115] N. Kishida, S. Matsuda, O. Itano, M. Shinoda, M. Kitago, H. Yagi, Y. Abe, T. Hibi, Y.
927 Masugi, K. Aiura, M. Sakamoto, Y. Kitagawa, Development of a novel mouse model of
928 hepatocellular carcinoma with nonalcoholic steatohepatitis using a high-fat, choline-
929 deficient diet and intraperitoneal injection of diethylnitrosamine, BMC Gastroenterol 16
930 (2016) 61.
931 [116] J.Q. Liang, N. Teoh, L. Xu, S. Pok, X. Li, E.S.H. Chu, J. Chiu, L. Dong, E. Arfianti, W.G.
932 Haigh, M.M. Yeh, G.N. Ioannou, J.J.Y. Sung, G. Farrell, J. Yu, Dietary cholesterol
933 promotes steatohepatitis related hepatocellular carcinoma through dysregulated
934 metabolism and calcium signaling, Nat Commun 9 (2018) 4490.
935 [117] M. Obradovic, E. Sudar-Milovanovic, S. Soskic, M. Essack, S. Arya, A.J. Stewart, T.
936 Gojobori, E.R. Isenovic, Leptin and Obesity: Role and Clinical Implication, Front

937 Endocrinol (Lausanne) 12 (2021) 585887.

938 [118] F. Suriano, S. Vieira-Silva, G. Falony, M. Roumain, A. Paquot, R. Pelicaen, M. Regnier,
939 N.M. Delzenne, J. Raes, G.G. Muccioli, M. Van Hul, P.D. Cani, Novel insights into the
940 genetically obese (ob/ob) and diabetic (db/db) mice: two sides of the same coin,
941 Microbiome 9 (2021) 147.

942 [119] E.J. Park, J.H. Lee, G.Y. Yu, G. He, S.R. Ali, R.G. Holzer, C.H. Osterreicher, H.
943 Takahashi, M. Karin, Dietary and genetic obesity promote liver inflammation and
944 tumorigenesis by enhancing IL-6 and TNF expression, Cell 140 (2010) 197-208.

945 [120] L.H. Tetri, M. Basaranoglu, E.M. Brunt, L.M. Yerian, B.A. Neuschwander-Tetri, Severe
946 NAFLD with hepatic necroinflammatory changes in mice fed trans fats and a high-
947 fructose corn syrup equivalent, Am J Physiol Gastrointest Liver Physiol 295 (2008)
948 G987-995.

949 [121] J.K. Dowman, L.J. Hopkins, G.M. Reynolds, N. Nikolaou, M.J. Armstrong, J.C. Shaw,
950 D.D. Houlihan, P.F. Lalor, J.W. Tomlinson, S.G. Hubscher, P.N. Newsome,
951 Development of hepatocellular carcinoma in a murine model of nonalcoholic
952 steatohepatitis induced by use of a high-fat/fructose diet and sedentary lifestyle, Am J
953 Pathol 184 (2014) 1550-1561.

954 [122] M. Fujii, Y. Shibazaki, K. Wakamatsu, Y. Honda, Y. Kawauchi, K. Suzuki, S. Arumugam,
955 K. Watanabe, T. Ichida, H. Asakura, H. Yoneyama, A murine model for non-alcoholic
956 steatohepatitis showing evidence of association between diabetes and hepatocellular
957 carcinoma, Med Mol Morphol 46 (2013) 141-152.

958 [123] K. Saito, T. Uebanso, K. Maekawa, M. Ishikawa, R. Taguchi, T. Nammo, T. Nishimaki-

959 Mogami, H. Udagawa, M. Fujii, Y. Shibazaki, H. Yoneyama, K. Yasuda, Y. Saito,
960 Characterization of hepatic lipid profiles in a mouse model with nonalcoholic
961 steatohepatitis and subsequent fibrosis, Sci Rep 5 (2015) 12466.
962 [124] K. Takakura, S. Koido, M. Fujii, T. Hashiguchi, Y. Shibazaki, H. Yoneyama, H. Katagi,
963 M. Kajihara, T. Misawa, S. Homma, T. Ohkusa, H. Tajiri Characterization of Non-
964 Alcoholic Steatohepatitis-derived Hepatocellular Carcinoma as a Human Stratification
965 Model in Mice, Anticancer Res. 34 (2014) 4849-4855.
966 [125] H. Yang, Q. Deng, T. Ni, Y. liu, L. Lu, H. Dai, H. Wang, W. Yang, Targeted Inhibition of
967 LPL/FABP4/CPT1 fatty acid metabolic axis can effectively prevent the progression of
968 nonalcoholic steatohepatitis to liver cancer, International Journal of Biological Sciences
969 17 (2021) 4207-4222.
970 [126] A. Asgharpour, S.C. Cazanave, T. Pacana, M. Seneshaw, R. Vincent, B.A. Banini, D.P.
971 Kumar, K. Daita, H.K. Min, F. Mirshahi, P. Bedossa, X. Sun, Y. Hoshida, S.V. Koduru,
972 D. Contaifer, Jr., U.O. Warncke, D.S. Wijesinghe, A.J. Sanyal, A diet-induced animal
973 model of non-alcoholic fatty liver disease and hepatocellular cancer, J Hepatol 65 (2016)
974 579-588.
975 [127] H. Nakagawa, A. Umemura, K. Taniguchi, J. Font-Burgada, D. Dhar, H. Ogata, Z.
976 Zhong, M.A. Valasek, E. Seki, J. Hidalgo, K. Koike, R.J. Kaufman, M. Karin, ER stress
977 cooperates with hypernutrition to trigger TNF-dependent spontaneous HCC
978 development, Cancer Cell 26 (2014) 331-343.
979 [128] C. Lebeaupin, D. Vallee, Y. Hazari, C. Hetz, E. Chevet, B. Bailly-Maitre, Endoplasmic
980 reticulum stress signalling and the pathogenesis of non-alcoholic fatty liver disease, J

Hepatol 69 (2018) 927-947.

[129] H.K. Seitz, R. Bataller, H. Cortez-Pinto, B. Gao, A. Gual, C. Lackner, P. Mathurin, S. Mueller, G. Szabo, H. Tsukamoto, Alcoholic liver disease, Nat Rev Dis Primers 4 (2018) 16.

[130] R. Teschke, Hepatocellular carcinoma in alcoholic liver disease: mechanistic considerations and clinical facts, Hepatoma Research 2019 (2019).

[131] H.K. Seitz, F. Stickel, Acetaldehyde as an underestimated risk factor for cancer development: role of genetics in ethanol metabolism, Genes Nutr 5 (2010) 121-128.

[132] Y. Sun, Q. Wang, Y. Zhang, M. Geng, Y. Wei, Y. Liu, S. Liu, R.B. Petersen, J. Yue, K. Huang, L. Zheng, Multigenerational maternal obesity increases the incidence of HCC in offspring via miR-27a-3p, J Hepatol 73 (2020) 603-615.

[133] H. Fu, B. Tang, J. Lang, Y. Du, B. Cao, L. Jin, M. Fang, Z. Hu, C. Cheng, X. Liu, Q. Shou, High-Fat Diet Promotes Macrophage-Mediated Hepatic Inflammation and Aggravates Diethylnitrosamine-Induced Hepatocarcinogenesis in Mice, Front Nutr 7 (2020) 585306.

[134] J. Gao, R. Xiong, D. Xiong, W. Zhao, S. Zhang, T. Yin, X. Zhang, G. Jiang, Z. Yin, The Adenosine Monophosphate (AMP) Analog, 5-Aminoimidazole-4-Carboxamide Ribonucleotide (AICAR) Inhibits Hepatosteatosis and Liver Tumorigenesis in a High-Fat Diet Murine Model Treated with Diethylnitrosamine (DEN), Med Sci Monit 24 (2018) 8533-8543.

[135] A.S. Arboatti, F. Lambertucci, M.G. Sedlmeier, G. Pisani, J. Monti, M.L. Alvarez, D.E.A. Frances, M.T. Ronco, C.E. Carnovale, Diethylnitrosamine enhances hepatic

tumorigenic pathways in mice fed with high fat diet (Hfd), Chem Biol Interact 303 (2019) 70-78.

[136] F. Gonzalez-Romero, D. Mestre, I. Aurrekoetxea, C.J. O'Rourke, J.B. Andersen, A. Woodhoo, M. Tamayo-Caro, M. Varela-Rey, M. Palomo-Irigoyen, B. Gomez-Santos, D.S. de Urturi, M. Nunez-Garcia, J.L. Garcia-Rodriguez, L. Fernandez-Ares, X. Buque, A. Iglesias-Ara, I. Bernales, V.G. De Juan, T.C. Delgado, N. Goikoetxea-Usandizaga, R. Lee, S. Bhanot, I. Delgado, M.J. Perugorria, G. Errazti, L. Mosteiro, S. Gaztambide, I. Martinez de la Piscina, P. Iruzubieta, J. Crespo, J.M. Banales, M.L. Martinez-Chantar, L. Castano, A.M. Zubiaga, P. Aspichueta, E2F1 and E2F2-Mediated Repression of CPT2 Establishes a Lipid-Rich Tumor-Promoting Environment, Cancer Res 81 (2021) 2874-2887.

[137] G. Cui, R.C. Martin, H. Jin, X. Liu, H. Pandit, H. Zhao, L. Cai, P. Zhang, W. Li, Y. Li, Up-regulation of FGF15/19 signaling promotes hepatocellular carcinoma in the background of fatty liver, J Exp Clin Cancer Res 37 (2018) 136.

[138] B. Wang, X. Li, W. Hu, Y. Zhou, Y. Din, Silencing of lncRNA SNHG20 delays the progression of nonalcoholic fatty liver disease to hepatocellular carcinoma via regulating liver Kupffer cells polarization, IUBMB Life 71 (2019) 1952-1961.

[139] J.M. Henderson, N. Polak, J. Chen, B. Roediger, W. Weninger, J.G. Kench, G.W. McCaughan, H.E. Zhang, M.D. Gorrell, Multiple liver insults synergize to accelerate experimental hepatocellular carcinoma, Sci Rep 8 (2018) 10283.

[140] X. Chao, S. Wang, M. Hlobik, A. Ballabio, H.M. Ni, W.X. Ding, Loss of Hepatic Transcription Factor EB Attenuates Alcohol-Associated Liver Carcinogenesis, Am J

Pathol (2021).

[141] J. Shi, S. Song, S. Li, K. Zhang, Y. Lan, Y. Li, TNF-alpha/NF-kappaB signaling epigenetically represses PSD4 transcription to promote alcohol-related hepatocellular carcinoma progression, Cancer Med 10 (2021) 3346-3357.

[142] J.Y. Lim, C. Liu, K.Q. Hu, D.E. Smith, D. Wu, S. Lamon-Fava, L.M. Ausman, X.D. Wang, Xanthophyll beta-Cryptoxanthin Inhibits Highly Refined Carbohydrate Diet-Promoted Hepatocellular Carcinoma Progression in Mice, Mol Nutr Food Res 64 (2020) e1900949.

[143] V. Ribas, L.C. de la Rosa, D. Robles, S. Nunez, P. Segales, N. Insausti-Urkia, E. Solsona-Vilarrasa, J.C. Fernandez-Checa, C. Garcia-Ruiz, Dietary and Genetic Cholesterol Loading Rather Than Steatosis Promotes Liver Tumorigenesis and NASH-Driven HCC, Cancers (Basel) 13 (2021).

[144] A. Ikawa-Yoshida, S. Matsuo, A. Kato, Y. Ohmori, A. Higashida, E. Kaneko, M. Matsumoto, Hepatocellular carcinoma in a mouse model fed a choline-deficient, L-amino acid-defined, high-fat diet, Int J Exp Pathol 98 (2017) 221-233.

[145] K. Rosania, Relying on chimpanzees for hepatitis research, Lab Anim (NY) 42 (2013) 188.

[146] K. Cho, S.W. Ro, S.H. Seo, Y. Jeon, H. Moon, D.Y. Kim, S.U. Kim, Genetically Engineered Mouse Models for Liver Cancer, Cancers (Basel) 12 (2019).

[147] C. Herrscher, P. Roingeard, E. Blanchard, Hepatitis B Virus Entry into Cells, Cells 9 (2020).

[148] P. An, J. Xu, Y. Yu, C.A. Winkler, Host and Viral Genetic Variation in HBV-Related

Hepatocellular Carcinoma, Front Genet 9 (2018) 261.

[149] J. Torresi, B.M. Tran, D. Christiansen, L. Earnest-Silveira, R.H.M. Schwab, E. Vincan, HBV-related hepatocarcinogenesis: the role of signalling pathways and innovative ex vivo research models, BMC Cancer 19 (2019) 707.

[150] K. Koike, K. Moriya, K. Iino, H. Yotsuyanagi, Y. Endo, T. Miyamura, T. Kurokawa, High-level expression of hepatitis B virus HBx gene and hepatocarcinogenesis in transgenic mice, Hepatology 19 (1994) 810-819.

[151] F.V. Chisari, P. Filippi, J. Buras, A. McLachlan, H. Popper, C.A. Pinkert, R.D. Palmiter, R.L. Brinster, Structural and pathological effects of synthesis of hepatitis B virus large envelope polypeptide in transgenic mice, Proc Natl Acad Sci U S A 84 (1987) 6909-6913.

[152] C.W. Kim, K.M. Chang, Hepatitis C virus: virology and life cycle, Clin Mol Hepatol 19 (2013) 17-25.

[153] Y. Hoshida, B.C. Fuchs, N. Bardeesy, T.F. Baumert, R.T. Chung, Pathogenesis and prevention of hepatitis C virus-induced hepatocellular carcinoma, J Hepatol 61 (2014) S79-90.

[154] Y. Kamegaya, Y. Hiasa, L. Zukerberg, N. Fowler, J.T. Blackard, W. Lin, W.H. Choe, E.V. Schmidt, R.T. Chung, Hepatitis C virus acts as a tumor accelerator by blocking apoptosis in a mouse model of hepatocarcinogenesis, Hepatology 41 (2005) 660-667.

[155] J.J. Morton, G. Bird, Y. Refaeli, A. Jimeno, Humanized Mouse Xenograft Models: Narrowing the Tumor-Microenvironment Gap, Cancer Res 76 (2016) 6153-6158.

[156] M. Yan, H. Li, F. Zhao, L. Zhang, C. Ge, M. Yao, J. Li, Establishment of NOD/SCID

mouse models of human hepatocellular carcinoma via subcutaneous transplantation of histologically intact tumor tissue, Chin J Cancer Res 25 (2013) 289-298.

[157] A. Labani-Motlagh, M. Ashja-Mahdavi, A. Loskog, The Tumor Microenvironment: A Milieu Hindering and Obstructing Antitumor Immune Responses, Front Immunol 11 (2020) 940.

[158] M. Yao, J. Hu, M. Daniels, H. Yien, H. Lu, H. Sharan, X. Zhou, Z. Zeng, T. Li, Y. Yang, A.R. Hoffman, A Novel Orthotopic Tumor Model to Study Growth Factors and Oncogenes in Hepatocarcinogenesis, Clinical Cancer Research 9 (2003) 2719-2726.

[159] S. Hajighasemlou, S. Pakzad, J. Ai, S. Muhammadnejad, M. Mirmoghtadaei, F. Hosseinzadeh, S. Gharibzadeh, A. Kamali, A. Ahmadi, J. Verdi, Characterization and Validation of Hepatocellular Carcinoma (HCC) Xenograft tumor as a Suitable Liver Cancer Model for Preclinical Mesenchymal Stem Cell Studies, Asian Pac J Cancer Prev 19 (2018) 1627-1631.

[160] E. Bresnahan, P. Ramadori, M. Heikenwalder, L. Zender, A. Lujambio, Novel patient-derived preclinical models of liver cancer, J Hepatol 72 (2020) 239-249.

[161] X. Qi, E. Schepers, D. Avella, E.T. Kimchi, J.T. Kaifi, K.F. Staveley-O'Carroll, G. Li, An Oncogenic Hepatocyte-Induced Orthotopic Mouse Model of Hepatocellular Cancer Arising in the Setting of Hepatic Inflammation and Fibrosis, J. Vis. Exp. (2019).

[162] V. Hernandez-Gea, S. Toffanin, S.L. Friedman, J.M. Llovet, Role of the microenvironment in the pathogenesis and treatment of hepatocellular carcinoma, Gastroenterology 144 (2013) 512-527.

[163] T. Wu, E. Heuillard, V. Lindner, G. Bou About, M. Ignat, J.P. Dillenseger, N. Anton, E.

1091 Dalimier, F. Gosse, G. Foure, F. Blindauer, C. Giraudeau, H. El-Saghire, M. Bouhadjar,
1092 C. Calligaro, T. Sorg, P. Choquet, T. Vandamme, C. Ferrand, J. Marescaux, T.F.
1093 Baumert, M. Diana, P. Pessaux, E. Robinet, Multimodal imaging of a humanized
1094 orthotopic model of hepatocellular carcinoma in immunodeficient mice, Sci Rep 6 (2016)
1095 35230.
1096 [164] W. Xu, Z.Y. Zhao, Q.M. An, B. Dong, A. Lv, C.P. Li, X.Y. Guan, X.Y. Tian, J.H. Wu,
1097 C.Y. Hao, Comprehensive comparison of patient-derived xenograft models in
1098 Hepatocellular Carcinoma and metastatic Liver Cancer, Int J Med Sci 17 (2020) 3073-
1099 3081.
1100 [165] S. Nuciforo, I. Fofana, M.S. Matter, T. Blumer, D. Calabrese, T. Boldanova, S.
1101 Piscuoglio, S. Wieland, F. Ringnalda, G. Schwank, L.M. Terracciano, C.K.Y. Ng, M.H.
1102 Heim, Organoid Models of Human Liver Cancers Derived from Tumor Needle Biopsies,
1103 Cell Rep 24 (2018) 1363-1376.
1104 [166] Y. Wu, J. Wang, X. Zheng, Y. Chen, M. Huang, Q. Huang, W. Xiao, H. Wei, Z. Tian, R.
1105 Sun, C. Sun, Establishment and Preclinical Therapy of Patient-derived Hepatocellular
1106 Carcinoma Xenograft Model, Immunol Lett 223 (2020) 33-43.
1107 [167] B.C. Bock, U. Stein, C.A. Schmitt, H.G. Augustin, Mouse models of human cancer,
1108 Cancer Res 74 (2014) 4671-4675.
1109 [168] H. Xin, K. Wang, G. Hu, F. Xie, K. Ouyang, X. Tang, M. Wang, D. Wen, Y. Zhu, X. Qin,
1110 Establishment and characterization of 7 novel hepatocellular carcinoma cell lines from
1111 patient-derived tumor xenografts, PLoS One 9 (2014) e85308.
1112 [169] E. Bresnahan, K.E. Lindblad, M. Ruiz de Galarreta, A. Lujambio, Mouse Models of

Oncoimmunology in Hepatocellular Carcinoma, Clin Cancer Res 26 (2020) 5276-5286.

[170] Q. Chen, J. Wang, W.N. Liu, Y. Zhao, Cancer Immunotherapies and Humanized Mouse Drug Testing Platforms, Transl Oncol 12 (2019) 987-995.

[171] Q. Zhou, J. Facciponte, M. Jin, Q. Shen, Q. Lin, Humanized NOD-SCID IL2rg-/- mice as a preclinical model for cancer research and its potential use for individualized cancer therapies, Cancer Lett 344 (2014) 13-19.

[172] Y. Choi, S. Lee, K. Kim, S.H. Kim, Y.J. Chung, C. Lee, Studying cancer immunotherapy using patient-derived xenografts (PDXs) in humanized mice, Exp Mol Med 50 (2018) 1-9.

[173] E.M. Wilson, J. Bial, B. Tarlow, G. Bial, B. Jensen, D.L. Greiner, M.A. Brehm, M. Grompe, Extensive double humanization of both liver and hematopoiesis in FRGN mice, Stem Cell Res 13 (2014) 404-412.

Figure 1

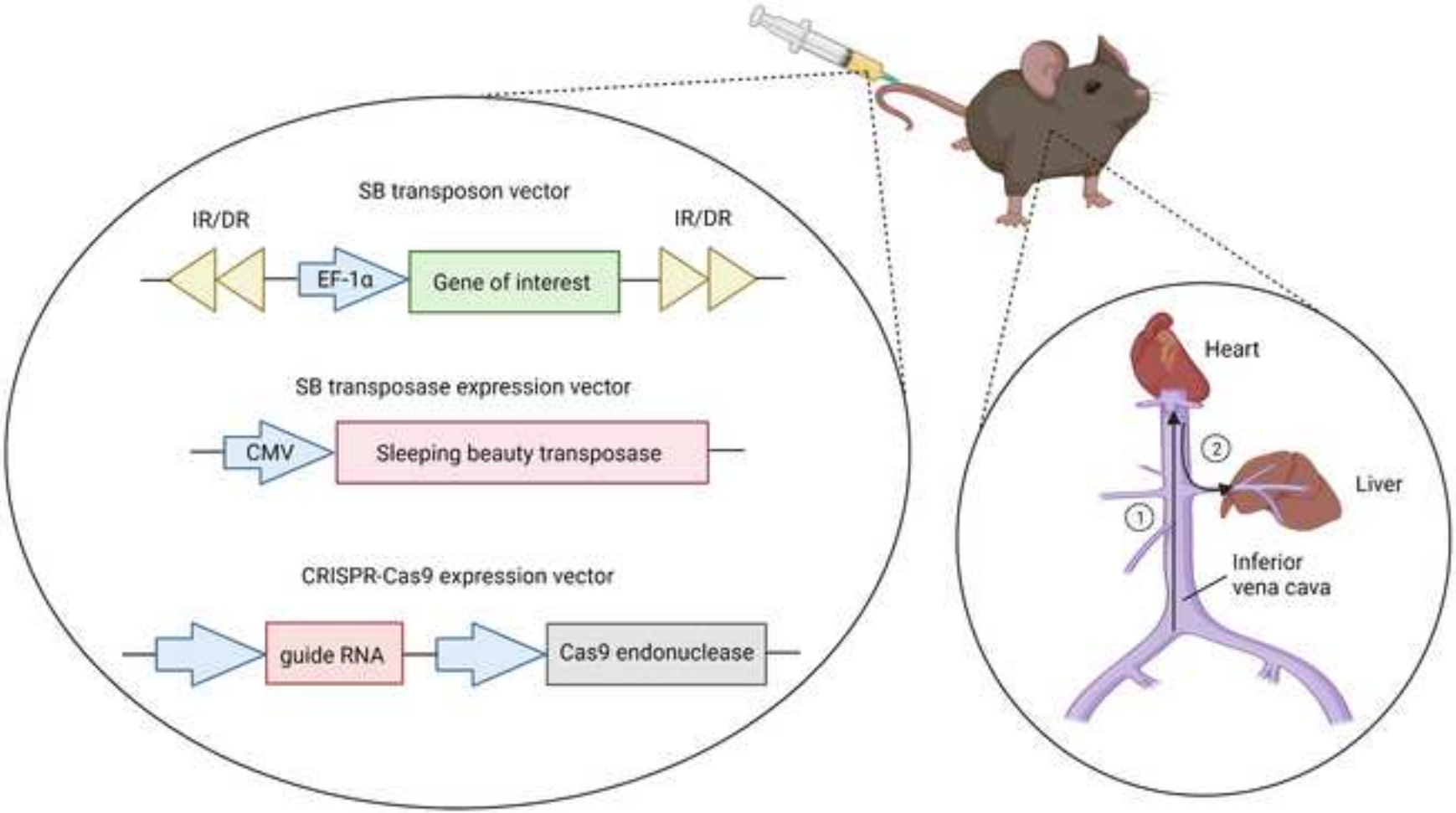

Gu et al., Figure 1

Figure 2

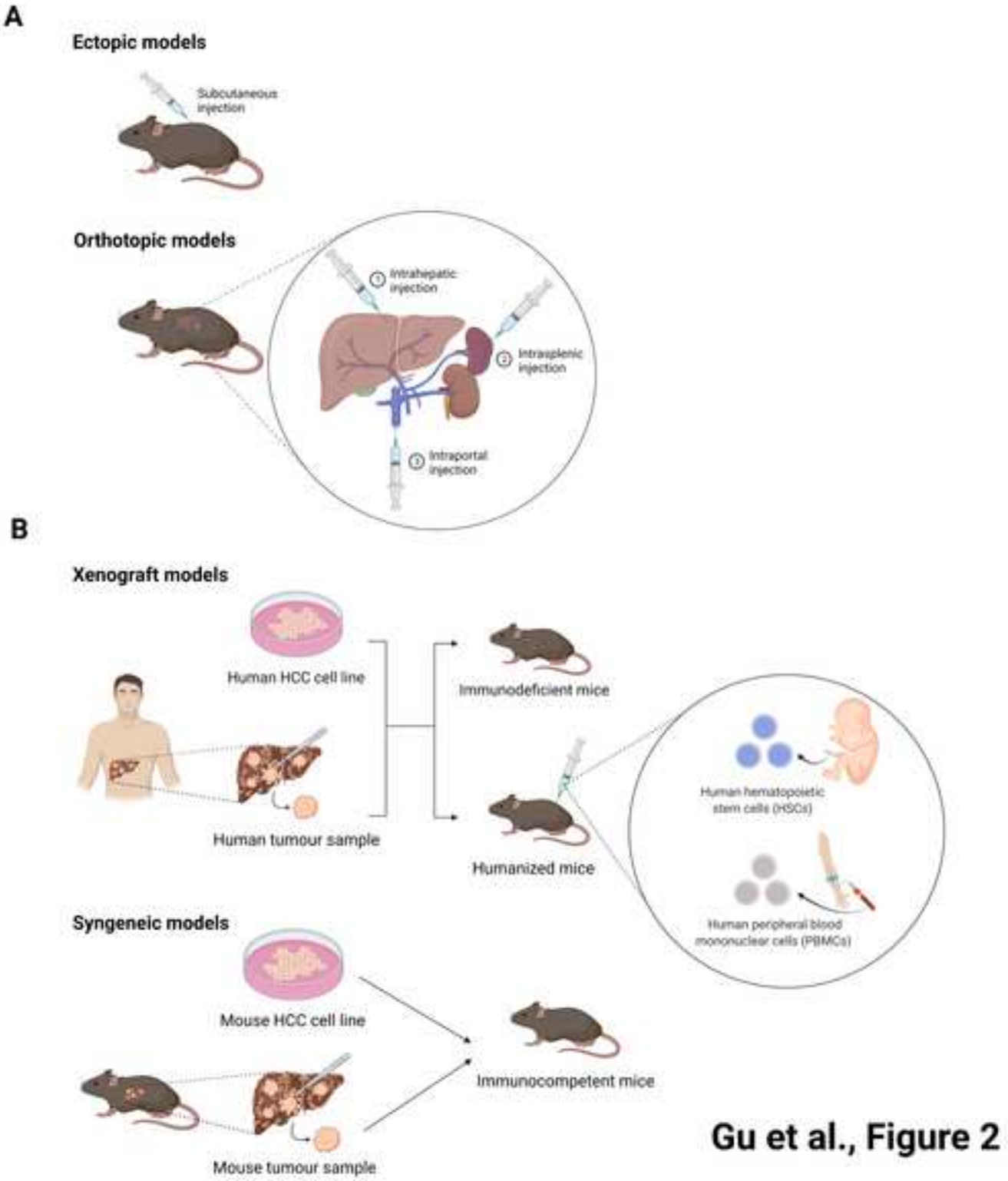

Figure 3

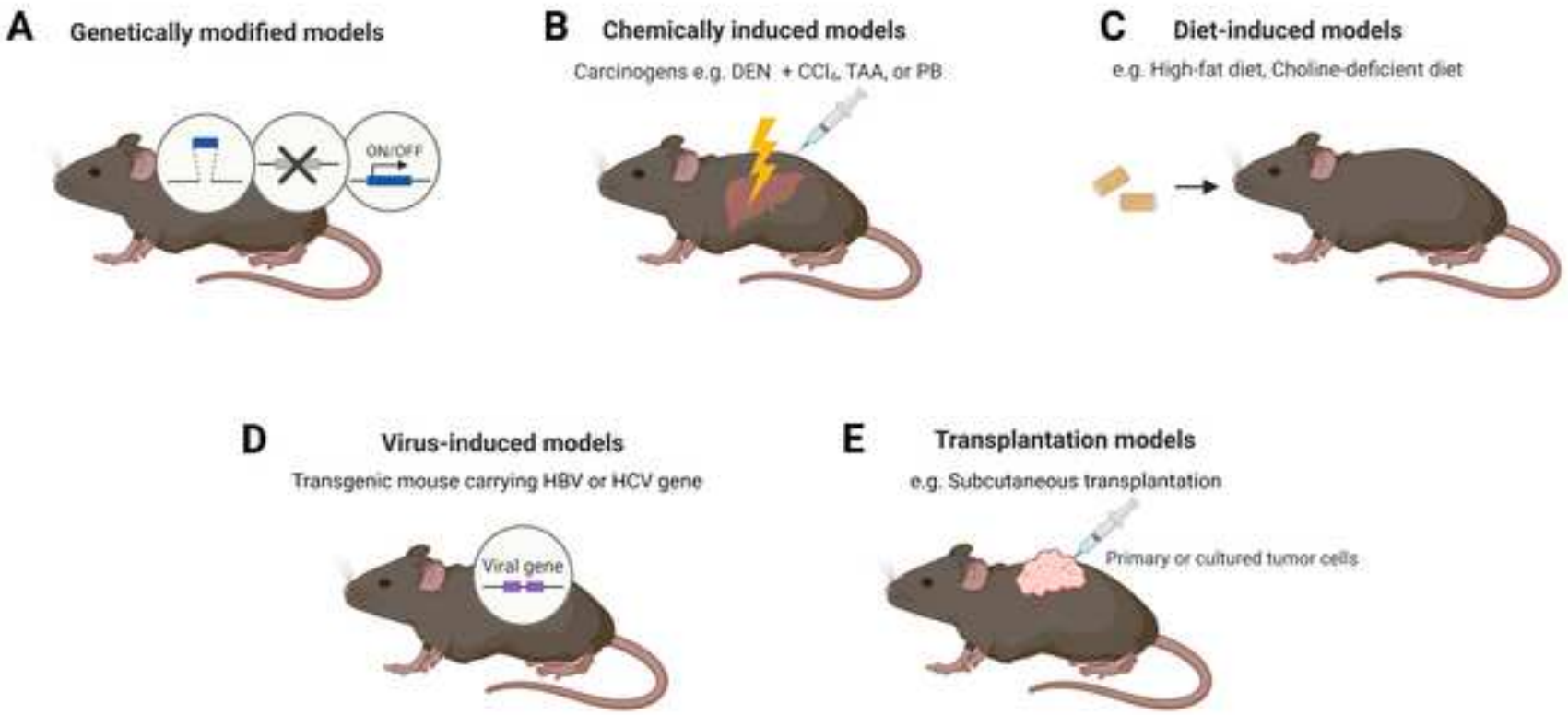

Gu et al., Figure 3

Table 1

Genetically modified mouse models generated using hydrodynamic tail vein injection.

Gene	Strain	Method	Time of HCC development	Reference
YAP	C57BL/6J	HTVI	~ 6 months (70% of mice)	Kamimura et al. [40]
c-Myc	FVB/N	SB transposase	~ 6 weeks	Cigliano et al. [41]
c-Met, myr-AKT	FVB/N	SB transposase	6-8 weeks (c-Met, myr-AKT) (lethal) 24 weeks (myr-AKT alone)	Hu et al. [42]
c-Met, myr-AKT	FVB/N	SB transposase	~ 6 weeks	Mo et al. [43]
c-Met, β-catenin^{S45Y}; c-Met, ΔN90-β-catenin	FVB/N	SB transposase	~ 7 weeks	Qiao et al. [44]
c-Met, β-catenin^{S45Y}	FVB/N	SB transposase	~ 5 weeks	Zhan et al. [45]
c-Met, ΔN90-β-catenin	C57BL/6J	SB transposase	~ 8 weeks	Li et al. [46]
hMet, β-catenin^{S45Y}; hMet, β-catenin^{S33Y}	FVB	SB transposase	6-9 weeks	Tao et al. [47]
myr-AKT, NRas	C57BL/6J	SB transposase	Day 45 (80% of mice), Day 58 (100% of mice)	Liu et al. [48]
RBMY, myr-AKT, NRasV12	FVB	SB transposase	~ 8 weeks	Kido et al. [49]
TAZ^{S89A}, HRAS^{G12V}	C57BL/6	SB transposase	~ 5 weeks	Cho et al. [50]
c-Myc, shp53	C57BL/6	SB transposase	~ 7 months (43.5% of mice)	Chung et al. [26]
Pten-KO, NRas	CD-1	NRas (SB transposase), Pten-KO (CRISPR/Cas9)	~ 16 weeks	Gao et al. [51]
c-Myc, Trp53-KO	C57BL/6	Trp53-KO (CRISPR-Cas9), c-Myc (SB transposase)	3-5 weeks	Chiu et al. [52]
c-Myc, Pten-KO; c-Myc, p53-KO	C57BL/6N	p53-KO & Pten-KO (CRISPR-Cas9), c-Myc (SB transposase)	Day 44 (c-Myc, Pten-KO), Day 28 (c-Myc, p53-KO)	Lee et al. [53]
c-Met, Pten-KO	FVB/N	Pten-KO (CRISPR-Cas9), c-Myc (SB transposase)	~ 9 weeks	Xu et al. [54]
c-Met, ΔN90-β-catenin, pT3-Cre	TBX3$^{flox/flox}$	Cre-loxP	~ 6 weeks	Liang et al. [38]
myr-AKT, pT3-Cre	FASN$^{fl/fl}$	Cre-loxP	22-28 weeks (only control)	Li et al. [55]
c-Met, myr-AKT, pT3-Cre	FASN$^{fl/fl}$	Cre-loxP	~ 8 weeks (only control) (lethal)	Hu et al. [42]
c-Met, β-catenin, pT3-Cre	FASN$^{fl/fl}$	Cre-loxP	~ 8 weeks (lethal)	Che et al. [56]

HTVI: Hydrodynamic tail vein injection; SB transposase: *Sleeping beauty* transposase; YAP: Yes-associated protein; RBMY: RNA-binding motif gene on Y chromosome; TAZ:

Transcriptional coactivator with PDZ-binding motif; shp53: p53 short hairpin RNA; Trp53-KO: p53-knockout.

Table 2

Chemically induced mouse models generated using genotoxic and/or non-genotoxic carcinogens

Chemicals	Mouse strain (gender)	Age	Dose of chemicals	Administration route and frequency	Time of HCC development	Reference
DEN	Trem-2$^{-/-}$ mice on the C57BL/6 background (male)	15 days	30 mg/kg	Single i.p. injection	< 30-40 weeks after DEN injection	Esparza-Baquer et al. [84]
	GAPDH transgenic mice on the C57BL/6J background (male)	2 weeks	25 mg/kg		< 36 weeks	Liu et al. [85]
	C3H/HeOuJ mice (male)	14-16 days	20 mg/kg		< 40 weeks after DEN injection	Connor et al. [64]
	c-fos$^{hep\text{-}tetOFF}$ mice on the C57BL/6 background	5 weeks	100 mg/kg		< 7 months after DEN injection	Bakiri et al. [86]
	c-fos$^{\Delta li}$ mice on a mixed C57BL/6 × 129sv background	15 days	25 mg/kg		< 8 months after DEN injection	
	Hepatocyte-specific FTO-knockout (FTO$^{L\text{-}KO}$) mice on the C57/BL6N background (male)	15 days	25 mg/kg		< 8 months after DEN injection	Mittenbuhler et al. [87]
	Hepatocyte-specific Ptpn6-knockout (Ptpn6^{HKO}) mice (male)	15 days	25 mg/kg		< 11 months	Wen et al. [88]
	C57BL/6 mice (male)	Once the mice are obtained	165 mg/kg in sesame oil	DEN: oral administration, once a week for 10 weeks	< 30 weeks	Tang et al. [63]
DEN+CCl_4	NOD2$^{-/-}$ mice (male)	6 weeks	100 mg/kg DEN; 0.5 ml/kg CCl_4	DEN: single i.p. injection; CCl_4: 12 i.p. injections	< 24 weeks after DEN injection	Ma et al. [89]
	Gstz1$^{-/-}$ mice	2 weeks (75 mg/kg DEN), 3 weeks (2 ml/kg CCl_4);		DEN: two doses of i.p. injections;	< 32 weeks	Li et al. [90]

		20 weeks (50 mg/kg DEN)		CCl_4: twice a week for 12 weeks		
	Hepatocyte-specific Nod2-knockout ($Nod2^{\triangle hep}$) mice (male)	14-16 days	25 mg/kg DEN; 1.2 ml/kg CCl_4 (1:4 diluted with olive oil)	DEN: single i.p. injection; CCl_4: 8 biweekly i.p. injections for 4 weeks after the DEN injection	< 8 months after DEN injection	Zhou et al. [91]
	C3H/HeJ mice (male & female)	2 weeks (DEN); week 8-16 (CCl_4)	10 or 50 mg/kg DEN; 0.25-1.50 mL/kg CCl_4 (10% solution in corn oil)	DEN: single i.p. injection; CCl_4: 8 weekly i.p. injections	< 17 weeks	Romualdo et al. [92]
DEN + TAA	C57BL/6 mice	2 weeks (DEN 20 mg/kg), 3 weeks (DEN 30 mg/kg), 4-9 weeks (DEN 50 mg/kg); 10-18 weeks (TAA 300 mg/kg)		DEN: eight weekly i.p. injections; TAA: biweekly i.p. injections	< 24 weeks after first DEN injection	Memon et al. [93]
DEN + PB	$TRIM21^{+/+}$, $TRIM21^{+/-}$, $TRIM21^{-/-}$ mice on the C57BL/6J background (male)	14 days (DEN); 21 days (PB)	5 mg/kg DEN; 0.05% PB in drinking water	DEN: single i.p. injection; PB: oral administration 7 days after the DEN injection	< 10 months	Wang et al. [94]
	BALB/c mice (male)	15 days (DEN); 28 days (PB)	50 mg/kg DEN; 500 mg/L PB in drinking water	DEN: single i.p. injection; PB: oral administration for 12 weeks	< 28 days after DEN/PB treatment	Gani et al. [95]
	C57BL/6 mice (female)	8-10 weeks	20 mg/kg DEN; 0.05% PB in diet	DEN: single i.p. injection; PB: oral administration	< 52 weeks after DEN/PB treatment	Zhang et al. [96]
DEN+2-AAF	Albino rats (male)	15 days	200 mg/kg DEN; 0.03% 2-AAF dissolved in corn oil in diet	DEN: single i.p. injection; 2-AAF: oral administration for 18 weeks	< 21 weeks	Aly et al. [97]
DEN+2-AAF+ a partial (2/3) hepatectomy	Sprague-Dawley rats (male)	6 weeks	200 mg/kg DEN, 0.015% 2-AAF	DEN: single i.p. injection; 2-AAF: daily intragastric administration for 3 days at 2 weeks after the DEN injection and for 1 week at 3 days after hepatectomy.	< 7 weeks after hepatectomy	Shi et al. [98]

DEN: Diethylnitrosamine; CCl_4: Carbon tetrachloride; TAA: Thioacetamide; PB: Phenobarbital; 2-AAF: 2-acetylaminofluorene; i.p.: intraperitoneal; GAPDH: Glyceraldehyde 3-phosphate dehydrogenase; FTO: Fat mass and obesity-associated; PTPN6: Protein tyrosine phosphatase non-receptor type 6; NOD2: Nucleotide-binding oligomerization domain-containing protein 2; GSTZ1: Glutathione S-Transferase Zeta 1; TRIM21: Tripartite motif containing-21.

Table 3

NASH/ALD-associated HCC mouse models induced by a combination of diet, alcohol and/or chemotoxin

Model	Strain (gender)	Diet administration	Hepatotoxin administration	Time of HCC development	Reference
DEN + HFD	C57BL/6 mice (male and female)	HFD (60% kcal fat), female mice: 1-3 months; male mice: after weaning	25 mg/kg DEN i.p. injection at 15 days old (male mice)	< 40 weeks	Sun et al. [132]
	C3H mice (male)	HFD (5% shortening, 5% lard, and 1% cholesterol)	30 mg/mL DEN in drinking water	< 22 weeks	Fu et al. [133]
	C57BL/6 mice (male)	HFD (60% fat, 20% carbohydrate, and 20% protein) from six weeks old	25 mg/kg DEN i.p. injection at 2 weeks old	< 8 months	Gao et al. [134]
	C57BL/6 mice (male)	HFD (40% high fat) beginning at 5 weeks old for 41 weeks	75 mg/kg DEN i.p. injection at 21 weeks old	< 46 weeks	Arboatti et al. [135]
	E2f1 KO ($E2f1^{-/-}$), E2f2 KO ($E2f2^{-/-}$), WT mice on a mixed C57BL/6J and 129/Sv background (male)	one month after weaning, HFD for 32 weeks	25 mg/kg DEN i.p. injection at 14 days old	< 9 months	Gonzalez-Romero et al. [136]
	C57L/J mice (male)	HFD (60% kcal% fat) beginning at 4 weeks old	40 mg/kg DEN i.p. injection at 15 days old	< 6 months	Cui et al. [137]
	BALB/c mice (male)	HFD (20% protein, 42% fat, and 38% carbohydrates) from 1 week old to 36 weeks old	0.95 g/mL DEN in sterile water (17-32 weeks old); 45 mg/kg DEN i.p. injections once a week (33-36 weeks old)	< 36 weeks	Wang et al. [138]
DEN+ TAA+HFD	C57BL/6J mice (male)	HFD (45% fat, 20% protein, and 35% carbohydrates) beginning at 4 weeks old	25 mg/kg DEN i.p. injection at 14 days old; 300 mg/L TAA in drinking water from week 4	< 24 weeks (83%)	Henderson et al. [139]
DEN + WD	liver-specific Tfeb-KO ($Tfeb^{flox/flox}$, Albumin-Cre+, L-Tfeb KO) mice on a C57BL/6N, C57BL/6J mixed background (male)	2 weeks after the DEN injection, WD (42% fat calories and 0.2% cholesterol) from 4 weeks old for 22 weeks or 34 weeks	10 mg/kg DEN i.p. injection at 2 weeks old	< 26 weeks or < 38 weeks	Chao et al. [140]
DEN + ethanol	hepatocyte-specific PSD4 OE ($TG^{Alb\text{-}PSD4}$) and WT mice	Liquid ethanol (5%) diet from 6.5 months old for 2.5 months	Ten 40 mg/kg DEN i.p. injections at 4-day intervals beginning at 2 months old	< 9 months	Shi et al. [141]

	(male and female)				
DEN + HRCD	$BCO1^{-/-}/BCO2^{-/-}$ DKO and WT mice on a C57BL/6J background (male)	HRCD (66.5% carbohydrates containing sucrose and maltodextrin) alone or HRCD + BCX (10 mg/kg diet) for 24 weeks	25 mg/kg DEN i.p. injection at 2 weeks old	< 30 weeks	Lim et al. [142]
HFHCD	C57BL/6J (male)	HFHC (60% calories from fat with added 0.5% cholesterol) beginning at 6 weeks old for 10 months	/	< 10 months	Ribas et al. [143]
HFD or HFHCD	MUP-uPA transgenic mice	HFD (60% calories from fat), or HFHC (identical to HFD with added 0.5% cholesterol) for 6 months	/	< 6 months	Ribas et al. [143]
WD + SW	DIAMOND mice: A stable isogenic cross between C57BL/6J and 129S1/SvImJ mice (male)	WD (42% kcal from fat with added 0.1% cholesterol) + high fructose-glucose solution (SW, 23.1 g/L d-fructose + 18.9 g/L d-glucose) beginning at 8-12 weeks old for 52 weeks	/	32-52 weeks (89% mice)	Asgharpour et al. [126]
CD + AHFD	male C57BL/6J mice	CD + AHF diet supplemented with 0.1% methionine from 6 weeks old for 60 weeks	/	~ 36 weeks	Ikawa-Yoshida et al. [144]

NASH: Nonalcoholic steatohepatitis; ALD: Alcoholic liver disease; HCC: Hepatocellular carcinoma; DEN: Diethylnitrosamine; TAA: Thioacetamide; HFD: High-fat diet; E2F1: E2F Transcription Factor 1; Tfeb: Transcription factor EB; PSD4: Pleckstrin and Sec7 Domain Containing 4; BCO1: Beta-Carotene Oxygenase 1; BCO2: Beta-Carotene Oxygenase 2; HRCD: Highly refined carbohydrate diet; CD: Choline-deficient diet; AHF: L-amino-acid-defined, high-fat diet; HFHCD: High-fat high-cholesterol diet; OE: Overexpression; BCX: Beta-cryptoxanthin; KO: Knockout; DKO: Double knockout; DIAMOND: Diet-induced animal model of nonalcoholic fatty liver disease; WD: Western diet; SW: Sugary water; MUP-uPA: Major urinary protein-urokinase plasminogen activator.

Table 4

Pros and cons of different transplantation models

Transplantation model	Advantages	Disadvantages
Ectopic	1. Simple to perform 2. Rapid development of visible tumors 3. Easy to monitor tumor growth 4. Inexpensive 5. Low intra-procedure mortality	1. Lack tumor-liver microenvironment interactions 2. Unable to develop metastasis
Orthotopic	1. Recapitulate the native tumor microenvironment, including immune cells and stroma tissue, which is relevant to liver pathology 2. Rapidly establish early-stage tumor growth 3. Model tumor metastasis and organ tropism	1. Require technically demanding surgery 2. Difficult to measure the tumor size and monitor tumor progression
Xenograft	1. Well represent tumor heterogeneity and genetic mutations of human HCC 2. Can study *in vitro* pre-treated cells	Immunocompromised mice lack major components of the immune system; cannot mimic the full anti-tumor immune response
Syngeneic	Immunocompetent mice with a fully functional immune system enable studies of tumor immunology and tests of immunotherapy for HCC	1. Difficult to interpret and predict how a mouse immune response translates back to humans 2. Might contain the bias of irrelevant mutations that only occur in murine HCC tumors
Humanized mice	Humanized mice with the ability to generate anti-cancer immune responses enable oncologic immunotherapy screening	1. Technically intensive; involve engrafting human immune system 2. Difficult to establish 3. Expensive

HCC: Hepatocellular carcinoma.

Table 5

Summary of five main preclinical mouse models of HCC

Mouse model	Timepoint	Advantages	Limitations
Genetically modified models (using HTVI technique)	5 – 9 weeks	Allow studies of investigating the role of specific genes involved in HCC development	1. Single gene mutation may not be efficient in inducing HCC; simultaneous activation of oncogene and inactivation of tumor suppressor gene could accelerate the process 2. Lack the development of fibrosis or cirrhosis in hepatocarcinogenesis
Chemically induced models	6 – 10 months	1. Can model underlying liver diseases such as chronic inflammation, fibrosis, and cirrhosis 2. Cost effective	1. Time of HCC development depends on the age, gender, strain, and administration dosage 2. Unpredictable genetic alterations of HCC tumor 3. Time consuming
Diet-induced models	6 – 9 months	Well recapitulate NASH- and ALD-driven HCC development	1. Only special diet administration may not be sufficient to induce HCC; carcinogen combined with special diet might be necessary 2. Time consuming
Virus-induced models	4 – 10 months	1. Can model HBV- or HCV- associated HCC tumorigenesis 2. Defined genetic alterations in an established line using transgenic mice	1. Expensive and time-consuming 2. Technically challenging and resource-demanding 3. Issue of embryonic lethality
Transplantation models	2 – 7 months	Allow studies using human HCC cell lines or patient-derived HCC tumor samples that carry unique genetic characteristics of original biopsies	The involvement of chronic liver injury in the process of hepatocarcinogenesis is omitted

HCC: Hepatocellular carcinoma; HTVI: Hydrodynamic tail vein injection; NASH: Nonalcoholic steatohepatitis; ALD: Alcoholic liver disease; HBV: Hepatitis B virus; HCV: Hepatitis C virus.